

# Nanoparticle Engineered Photocatalytic Paints: A Roadmap to Self-Sterilizing against the Spread of Communicable Diseases

Vijay S. Mohite <sup>1</sup>, Milind M. Darade <sup>2</sup>, Rakesh K. Sharma <sup>3</sup> and Shivaji H. Pawar <sup>2,4,\*</sup>

<sup>1</sup> Department of Physics, T. C. College, Baramati 413102, India; vs.mohite@tccollege.org

<sup>2</sup> Center for Interdisciplinary Research, D. Y. Patil Education Society, Deemed to be University, Kolhapur 416006, India; milind.darade04@gmail.com

<sup>3</sup> Department of Obstetrics & Gynecology, D. Y. Patil Medical College, Kolhapur 416006, India; drksharmaz@gmail.com

<sup>4</sup> Centre for Innovative and Applied Research (CIAR), T. C. College, Baramati 413102, India

\* Correspondence: shpawar1946@gmail.com

**Abstract:** Applications of visible-light photocatalytic engineered nanomaterials in the preparation of smart paints are of recent origin. The authors have revealed a great potential of these new paints for self-sterilizing of the surfaces in hospitals and public places simply with visible light exposure and this is reported for the first time in this review. A recent example of a communicable disease such as COVID-19 is considered. With all precautions and preventions taken as suggested by the World Health Organization (WHO), COVID-19 has remained present for a longer time compared to other diseases. It has affected millions of people worldwide and the significant challenge remains of preventing infections due to SARS-CoV-2. The present review is focused on revealing the cause of this widespread disease and suggests a roadmap to control the spread of disease. It is understood that the transmission of SARS-CoV-2 virus takes place through contact surfaces such as doorknobs, packaging and handrails, which may be responsible for many preventable and nosocomial infections. In addition, due to the potent transmissibility of SARS-CoV-2, its ability to survive for longer periods on common touch surfaces is also an important reason for the spread of COVID-19. The existing antimicrobial cleaning technologies used in hospitals are not suitable, viable or economical to keep public places free from such infections. Hence, in this review, an innovative approach of coating surfaces in public places with visible-light photocatalytic nanocomposite paints has been suggested as a roadmap to self-sterilizing against the spread of communicable diseases. The formulations of different nanoparticle engineered photocatalytic paints with their ability to destroy pathogens using visible light, along with the field trials are also summarized and reported in this review. The potential suggestions for controlling the spread of communicable diseases are also listed at the end of the review.

**Keywords:** photocatalytic surface coating; smart paints; TiO<sub>2</sub> nanoparticles; pathogenic disinfection; green synthesis

**Citation:** Mohite, V.S.;

Darade, M.M.; Sharma, R.K.;

Pawar, S.H. Nanoparticle

Engineered Photocatalytic Paints: A

Roadmap to Self Sterilizing against

the Spread of Communicable

Diseases. *Catalysts* **2022**, *12*, 326.

<https://doi.org/10.3390/catal12030326>

Academic Editors: Roberto

Comparelli and Ilaria De Pasquale

Received: 10 January 2022

Accepted: 7 March 2022

Published: 11 March 2022

**Publisher's Note:** MDPI stays neutral with regard to jurisdictional claims in published maps and institutional affiliations.



**Copyright:**© 2022 by the authors.

Licensee MDPI, Basel, Switzerland.

This article is an open access article

distributed under the terms and

conditions of the Creative Commons

Attribution (CC BY) license

([http://creativecommons.org/licenses](http://creativecommons.org/licenses/by/4.0/)

[/by/4.0/](http://creativecommons.org/licenses/by/4.0/)).

## 1. Introduction

In recent years, the spread of communicable diseases has created great concern for societal health globally. The spread of the COVID-19 disease is a present example of communicable disease and it is so hazardous that the World Health Organization (WHO) has declared a pandemic. More worse than the severity of the disease is its persistence in the global community for longer than two years. It started in December 2019, still exists even after two years and its eradication is still unpredictable. In light of this situation, our research group which has been involved right from the inception of COVID-19 has taken up the initiative in fighting against this communicable disease based on the backgrounds of nanoscience and nanotechnology [1]. Even before the

emergence of COVID-19 disease, our group was working on communicable diseases such as tuberculosis [2–4]. The only difference is that tuberculosis is a microbial disease, while COVID-19 is a viral disease caused by SARS-CoV-2 virions (nanobiotic particles). Their methods of spreading and control do differ in principle.

Nanoparticles with significant anticorrosive and antipathogenic qualities have gained popularity in recent years and are in high demand when it comes to the composition of smart paints, which are designed to defend structures against biological and pathogenic attack. In densely populated and coastal places, pollutants and the marine atmosphere cause chemical or electrochemical corrosion. Nanomaterials are used as additives in smart paints since their coatings have great hydrophobicity and self-cleaning capabilities due to their photocatalytic activity [5–7]. This may help to reduce surface pollution by decomposing contaminants, hence improving the structural surface quality and look.

Antibacterial compounds are also increasingly being included in a number of coatings in specialized products with the purpose of inhibiting the growth of harmful germs on a variety of surfaces, which would improve the quality of life in both developed and developing countries. Antipathogenic nanoparticles in surface coatings may reduce the activity of a wide spectrum of Gram-positive and Gram-negative bacteria, which is difficult to prevent nowadays [8].

Titanium dioxide (TiO<sub>2</sub>) and zinc oxide (ZnO) nanoparticles doped with a variety of elements have been extensively studied for their applications as self-cleaning, anticorrosive and antibacterial additives in construction materials, especially in external surfaces, due to the improvement in the aesthetic quality of buildings as well as the reduction in maintenance costs [9–11].

Photocatalytic paints are self-cleaning since the slightest incident of light eliminates undesired substances on the surface. However, because its photocatalytic activity is not selective, the polymer paint matrix, as well as impurities, can be destroyed [12]. Most studies have focused on photocatalytic paints produced with anatase nanoparticles due to their high photocatalytic activity. When equally distributed in the film and exposed to light, nanoparticles with a large surface area, on the other hand, swiftly degrade the paint film surrounding them, resulting in photochalking [13].

As a result, the stability and photocatalytic activity of paint films are two critical elements to consider in the development of effective photocatalytic paints. In order for the paint to be effective without hastening the vehicle's deterioration, a balance must be struck between these two elements [14–16]. Many strategies have been offered to improve the stability of acrylic photocatalytic paints. One way to change the photocatalytic action of titanium dioxide is to change the particles shape and size. Because of their greater surface area and high crystallinity, which allows for greater light absorption, the mesoporous TiO<sub>2</sub> spheres stand out among the other TiO<sub>2</sub> morphologies known. Recently, porous TiO<sub>2</sub> microspheres with a large specific surface area were created and exploited in photovoltaic and photocatalytic applications [17,18].

In comparison to photocatalytic paints offering the advantages of TiO<sub>2</sub> nanoparticles, hierarchical structures in the form of mesoporous TiO<sub>2</sub> microspheres have been added to acrylic paint formulations to produce paints with superior photocatalytic properties and stability [19,20]. The advantage of using a photocatalyst with a large surface area but a micrometric diameter is that the active zone interacts with the paint surface much less, resulting in less photocatalytic degradation of the binder. Only experiments measuring photocatalytic activity and stability under high ageing conditions were conducted. It is also critical to test how smart paints behave in the environments where they may be used.

The majority of previous research has compared TiO<sub>2</sub> antibacterial efficiency to bacteria such as *E. coli*, which is commonly utilized as a test microorganism. Due to structural differences, such as the complexity and thickness of the cell membrane, fungi have been shown to have lower photocatalytic sensitivity than bacteria. Despite this, there are

currently no concentrated studies on fungal disinfection using photocatalysis [21]. Fungi are the most common microflora on painted surfaces and they can speed up the deterioration process. Furthermore, they can survive on the surface of the dirt or use the underlying substrate, causing allergies, respiratory problems, asthma and catastrophic health impacts in persons who have their immune systems weakened. Although various publications have tested the antifungal properties of photocatalytic paints using *Aspergillus niger* and non-pathogen molds as environmental models, these fungal species were not discovered on damaged paint surfaces, and are hence not regarded as paint degraders. Thus, there is some literature available on nanoparticle engineered smart paint coatings for anticorrosive and antifungal properties. However, very little data are available on photocatalytic disinfection with paint coatings for health-care applications [22,23]. Because nitrogen and oxygen have comparable ionic radii, nitrogen doping is a viable approach for modifying  $\text{TiO}_2$  because it requires less formation energy for substitution. Furthermore, the position of the N 2p state above the valence band narrows the bandgap and the band position is well aligned with respect to the redox potentials. To extend the absorption edge to visible light, nitrogen has been added to a variety of  $\text{TiO}_2$  nanostructures [24].

The proposed review is in continuation with our efforts towards “Fighting against the spread of COVID-19 disease caused due to the SARS-CoV-2 virus”. COVID-19 disease has persisted for a long time — more than 24 months since December 2019 and the main objective of this review is to reveal the ways and means of the spread of this communicable disease. It is likely that the spread might have been caused due to the existence of SARS-CoV-2 and its delta variant on the surfaces in public places such as lifts, door handles, transports, etc. Another objective of our review is to reveal the limitations of the existing antimicrobial cleaning technologies used in hospitals, which are not suitable, viable or economical to keep public places free from infections. In this situation, we have suggested and described in our review an additional approach of coating the surfaces at public places with visible-light-sensitive photocatalytic nanocomposite paints to disinfect the surfaces even with sunlight [25,26]. This is the roadmap that we have suggested at the end of our review, based on our research findings and the outcome of our project, entitled “Nanoparticle Engineered  $\text{TiO}_2$ -Based Photocatalytic Paint Surface Coatings for Pathogenic Disinfection” with the support of local Indian industries.

## 2. The Spread of Communicable Diseases: Ways and Means

A communicable disease is one that can be passed from one person to another through a variety of routes, including contact with blood and bodily fluids, inhalation of an airborne virus, or insect bite.

Case reporting is crucial for disease prevention and control program creation and evaluation, as well as the provision of appropriate medical treatment and the detection of common-source epidemics. California law requires healthcare practitioners and laboratories to report over 80 diseases and conditions to their local health department. Only a handful of the recognized communicable diseases include hepatitis A, B and C, influenza, measles, salmonella, food-borne infections and the recently emerging COVID-19 [27]. Depending on the nature of the pathogens, the communicable diseases are grouped into three different classes — viral, fungal and bacterial diseases — and are listed in Table 1.

**Table 1.** List of communicable diseases spread with different pathogens.

Sr.No	Viral Diseases	Fungal Diseases	Bacterial Diseases
1	2019-nCoV	Fungal nail infections	CRE
2	Ebola	Ring worm	MSRA
3	Enterovirus D68	Vaginal Candidiasis	Pertussis
4	Flu	Candida Infections of the mouth, throat & esophagus	Shigellosis
5	Hantavirus	-	Tuberculosis
6	Hepatitis A	-	-
7	Hepatitis B	-	-
8	HIV/AIDS	-	-
9	Measles	-	-
10	Rabies	-	-
11	Sexually Transmitted Disease	-	-
12	West Nile Virus	-	-
13	Zika	-	-

### 2.1. The Spread of Communicable Diseases

The disease or infectious agent in tissue determines the spread of communicable diseases. Infectious diseases can spread in a variety of ways, including:

1. Direct contact with an infected person, such as staphylococcus, gonorrhea, HIV, fecal/oral transmission (hepatitis A), or droplets (hepatitis B) (influenza, TB)
2. Contact with a Norwalk virus-infected surface or object, contaminated food (salmonella, *E. coli*), contaminated blood (HIV, hepatitis B), or contaminated water (HIV, hepatitis B) (cholera).
3. Disease-carrying insect or animal bites (mosquito bites cause malaria and yellow fever; flea bites cause plague).
4. Airborne infectious diseases such as tuberculosis and measles.

COVID-19 is the most recent example of the transmission of a communicable disease. It is transmitted through infectious agents such as SARS-CoV-2. This virus is only a few nanometers in size and cannot be seen with the naked eye, or even an optical microscope. It is also not a living entity, with no ability to regenerate. Nevertheless, its numbers have increased, resulting in a pandemic condition that has lasted for more than two years. This is primarily due to SARS-CoV-2's proliferation and long-term persistence. In the next sections, the rationale for the virus's propagation and the method of virus multiplication are discussed [28–30].

#### 2.1.1. Multiplication of the Virus (SARS CoV-2)

Viruses are non living entities that have a DNA or RNA core and a protective protein coating around them. They are one of the most diverse microorganism families, with 6590 species recognized by the International Committee on Taxonomy of Viruses. Viruses that infect humans usually have a size of 20 to 260 nanometers. However, certain viruses have the ability to proliferate to huge sizes [31–33]. The type and natures of viruses, as well as their life cycles, play a major role in their proliferation. The virus life cycles for SARS-CoV-2 are schematically described in Figure 1 and consist of distinct steps.

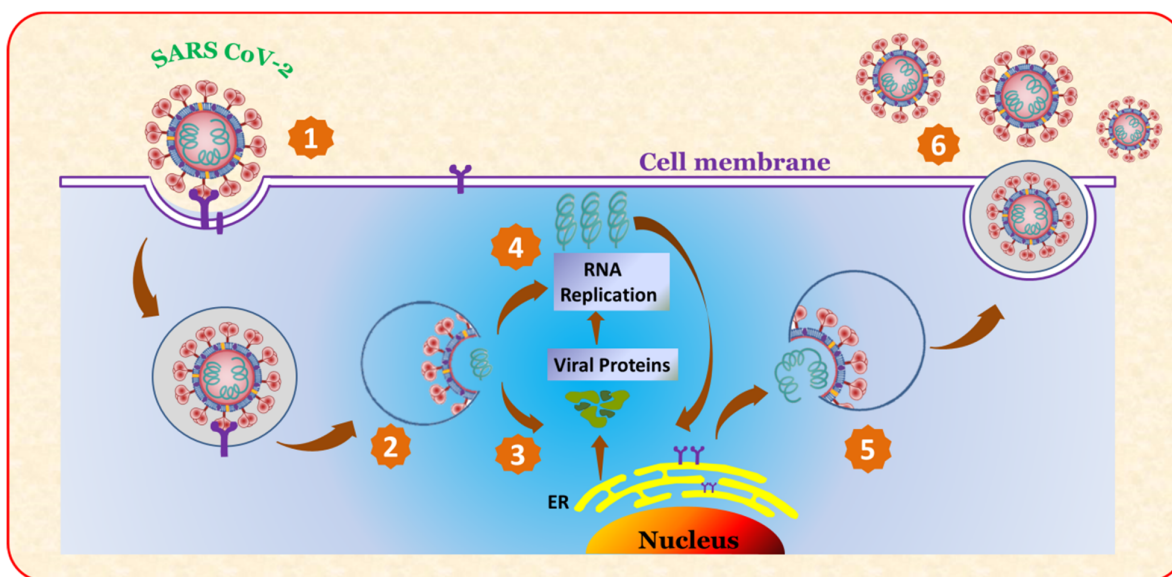


**Figure 1.** Principle of Multiplication of SARS-CoV-2 virus.

The virus SARS-CoV-2 grows at the cost of the human biological cell. The human cells are damaged one after another and large numbers of viruses are produced. The sequence of the damage to the cell producing viruses consists of six sequential steps: (1) The virion's spike protein interacts with ACE2, a cell-surface protein. TMPRSS2, an enzyme, aids virion entry. (2) The virion releases its RNA. (3) Some of this RNA is translated into proteins by the cell's machinery. (4) Some of these proteins form a replication complex to produce more RNA. (5) Proteins and RNA are assembled into a new virion in the Golgi and released. (6) Multiple production of viruses. [34,35].

The attachment and penetration of viruses, which is carried out by the virus capsid or envelope proteins, is the initial stage in their proliferation. Viruses replicate, reproduce, and discharge themselves using the machinery of the host cell. Retroviruses, for example, have their own replication enzyme (polymerase or reverse transcriptase), yet they are unable to multiply and proliferate outside of their host cell. Virion assembly begins once enough nucleic acids and proteins are present [36,37].

Virus multiplication is largely determined by the structure of the virus. As a result, it is critical to know what features it might have, such as infectivity, disinfectant susceptibility and replication mode. A virus is usually encased in a protective protein coating called a capsid. The role of the capsid is to safeguard the viral genome. They are generated in a very precise way. Capsids come in three different shapes: icosahedral, helical and complicated. Prokaryotic viruses have a prolate form, which is an elongated icosahedron. Capsid shapes are utilized to aid in virus identification and can reveal information about the virus' life cycle.

### 2.1.2. Transmission of Viruses

A variety of factors influence the spread of viral infections in a population. Age, structure, the availability of a new host and the transmission mechanism are all elements to consider. Some viruses can infect a wide range of animals, and cross-species transmission is also possible. Corona viruses, for example, have been found in a variety of birds and animals, including domestic cats and dogs. SARS-CoV, MERS-CoV, and COVID-19 are examples of human CoVoV that can cause respiratory failure [38–41].

Virus particles are typically transferred between humans through infected persons respiratory, cutaneous or other bodily fluid discharges. The virus can spread directly by aerosols and droplets, or indirectly through contact with contaminated surfaces. Viral contamination of fomites in a community could cause a variety of ailments. Norovirus (a

non-enveloped virus) is well known for its ability to survive for several weeks on a variety of surfaces, causing severe epidemics in healthcare facilities [42]. Aerosols and droplets can spread many respiratory viruses, including influenza and SARS-CoV. Aerosol transmission is usually thought to be the most dangerous, since it can spread infectious particles in high concentrations, with few infection control strategies available to halt it. As a result, understanding how long viruses may survive on a surface can help with the development of infection control strategies and the prevention of epidemics [43–45].

### 2.1.3. Persistence of Viruses

As the COVID-19 pandemic has continued for more than two years, the persistence of viruses has become a major worry. It is a complicated process that incorporates a variety of surface factors — structural, physical, biological and chemical. Since the discovery of the first virus in 1892, a lot of work has gone into understanding viral survival in different environments and determining the impact of surface characteristics on viral viability. Surface characteristics are influenced by factors such as porosity, topography, absorption, and surface hydrophobicity [46–48].

Effective antiviral surfaces may need to be customized to a specific virus type, since each type of virus interacts with a surface differently depending on its structure. Temperature, relative humidity, and how viruses permeate different surfaces are some of the other environmental parameters that influence viral persistence. These additional factors should be considered while developing an antiviral surface [49,50].

The surface parameters that influence virus persistence are schematically described in Figure 2. It may be seen in the diagram that there are four primary characteristics that influence virus persistence on surfaces: (i) physical, abiotic factors, such as relative humidity, temperature, and exposure to light; (ii) type of surface, e.g., roughness; (iii) biological, such as virus structure or the presence of other microorganisms, e.g., microbial biofilms; (iv) chemical, such as pH, presence of reactive ions, adsorption state, organic matter, or presence of specific substances. Many viruses can be sustained and protected by organic material in the environment, such as saliva or mucus droplets. It has been noted that the inclusion of bacteria, lipids and proteins in the viral inoculum can boost the persistence of viral inoculum on low-porosity surfaces such as plastic and stainless steel, as opposed to porous surfaces such as cardboard. The infectious SARS-CoV-2 virus was found to remain on the outer layer of a surgical mask after seven days, while no viable virus was found on treated flat stainless steel and plastic surfaces after seven days [51–53].

Here, an attempt has been made to some extent to understand the reason of long lasting persistence of COVID-19 by reviewing the persistence of SARS-CoV-2 on various matrices in different temperature and relative humidity conditions. The data collected from the literature are listed in Table 2. It may be noted that the persistence time of SARS-CoV-2 varies with the nature of the matrix, temperature and relative humidity. It is surprising to note that the SARS-CoV-2 virus persisted for about 21 days on plastics from face shields.

**Table 2.** Persistence of SARS-CoV-2 in/on different environmental matrices [54]

Sr. No	Matrix	Temp °C	Relative Humidity (%)	Persistence	100 % Decay Time	References
1	Tap water	RT	-	1.7 d	-	[55]
2	Cardboard	21–23	65	1 d	2 d	[56]
3	Copper	21–23	65	4 h	8 h	[56]
4	Stainless steel	21–23	65	3 d	4 d	[56]
5	Aerosol	RT	-	16 h	-	[57]
6	Cloth	22	65	1 d	2 d	[58]
7	Paper	22	65	30 min	3 d	[58]
8	Plastic	22	65	4 d	7 d	[58]

9	Cotton	20	35–40	1 h	4 h	[59]
10	Gloves (Nitrile)	20	35–40	7 d	7 d	[59]
11	Plastics from face shields	20	35–40	21 d	21 d	[59]
12	Tyvek	20	35–40	14 d	21 d	[59]
13	Cotton cloth	40	-	24 h	-	[60]
14	Stainless steel	19	57	7 d	-	[61]
15	Plastic (polypropylene)	27	65	1.5 h	-	[62]

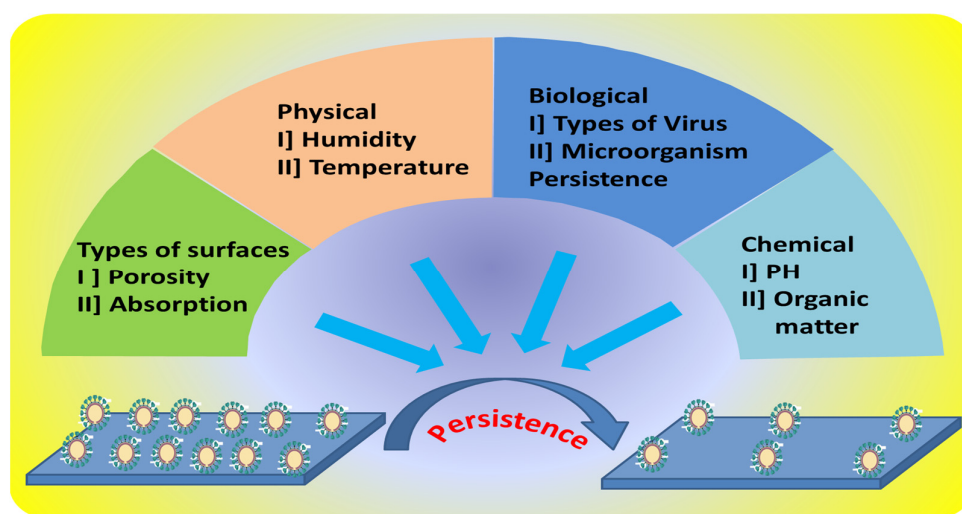


**Figure 2.** Surface properties influencing the persistence of viruses.

## 2.2. Controlling the Spread of Communicable Diseases with Disinfection of Pathogens

Pathogen disinfection is a crucial step to avoid the spread of communicable diseases. At the moment, this is mostly accomplished via traditional sterilization methods. However, there are significant limitations and downsides; thus, a new photocatalytic disinfection of pathogens approach is now being developed. In the following sections, we will discuss both traditional and new techniques.

### 2.2.1. Sterilization of Pathogens and Controlling the Spread of Communicable Diseases

Sterilization is a technique that uses physical or chemical methods to eradicate or eliminate all kinds of microbial life in health-care facilities. In order to prevent the spread of viruses such as SARS-CoV-2 and regulate the Covid-19 sickness, the WHO has given the following instructions: vaccinate yourself, wear a mask and keep a distance of at least 6 feet from others. Wash your hands frequently and avoid crowds and places with poor ventilation. Covering coughs and sneezes is a good idea. Clean and disinfect, keep an eye on your health every day. In order to prevent infectious microorganisms from being transmitted to patients, medical and surgical tools must be disinfected and sterilized [63]. Figure 3 shows a schematic representation of these strategies.





**Figure 3.** Present methods for controlling the spread of communicable diseases.

### 2.2.2. Sterilizing Surface Coatings to Work against the Spread of Communicable Diseases

The spread and persistence of communicable diseases such as COVID 19 have raised many challenges and threats to human society globally. One of the major challenges is the control of the spread of viruses and, in turn, communicable diseases. Some of the examples of applications of surface coatings for pathogenic disinfection are listed in Table 3.

The attachment of pathogens to the surface of a range of materials and devices, such as masks, gowns, clothes, utensils, furniture, frequently handled objects, personal protective equipment (PPE kits), glass, wood, paper and fabric is thought to be the main cause of pathogen dissemination. Doorknobs, stair railings, push plates, handles, drawer pulls, electrical switch plates, plumbing fittings, sinks and elevator floor buttons are all examples of biomedical affected devices. Self-sterilizing materials such as polypropylene, antiviral polymers, the inclusion of metal ions/oxides and functional nanoparticles, copper nanoparticles, metal oxide nanoparticles such as Ag, Au, Cu<sub>2</sub>O, TiO<sub>2</sub>, Fe<sub>3</sub>O<sub>4</sub>, and graphene are used to coat the surfaces of these substances. Surface coatings developed with these materials act as sterilizing agents and have a long shelf life. As a result, there will be no need for frequent cleaning, no risk of infection and it will be cost effective [64].

TiO<sub>2</sub> is the most widely used semiconductor because of its strong oxidizing ability, chemical stability, highly reactivity, ease of preparation, abundance, low cost, low toxicity, chemical inertness and long-term photostability [65].



**Table 3.** Examples of sterilizing surface coatings against the spread of communicable diseases

Sr. No	Application Type	Materials	References
1	Mask and PPE	Polypropylene	[66]
2	Mask, gowns and PPE	Antiviral polymers, incorporation of metal ions/oxides, and functional nanoparticles	[67]
3	Clothes, utensils, furniture, regularly touched objects and personal protective equipment	Copper nanoparticles	[68]
4	Coating, food packaging and textiles	Polymeric materials	[69]
5	Masks and protective clothing	Non-woven fabrics, metal-based Nanomaterials such as silver, copper, titanium, gold, and zinc)	[70]
6	Personal protective equipment (PPE)	Polyacrylonitrile (PAN)/zinc oxide (ZnO) hybrid nanocomposite	[71]
7	Glass, wood, paper and fabrics	Polymers, silver, TiO <sub>2</sub> , and copper-derived chemicals.	[72]
8	Biomedical devices and protective equipment of medical workers.	Cationic polymers, metal coatings and antifouling micro-/nanostructures	[73]
9	PPE, face masks, gowns, aprons and gloves	Antiviral Fabric	[74]
10	Medical gowns and drapes, PPE, mask or respirators,	N,N-dodecyl, methyl-polyurethane	[75]
11	Face masks	Metal oxide nanoparticles such as Ag, Au, Cu <sub>2</sub> O, TiO <sub>2</sub> , Fe <sub>3</sub> O <sub>4</sub>	[76]
12	Doorknobs, stair railings, push plates, handles, drawer pulls, electrical switch plates, plumbing fixtures and sinks, and elevator floor buttons	Copper (Cu) and its alloys	[77]
13	Masks	Silver, carbon nanotubes and titanium dioxide nanoparticles	[78]
14	PPE, masks	Copper oxide	[79]
15	Masks	Graphene	[80]
16	Healthcare workers include protective clothing, pathogenic microbes	Silver nanoparticles	[81]
17	Public transport system such as	Silver nanoparticles	[82]
18	Hospital applications	Aluminum 6063 alloy	[83]

### 3. Photocatalytic Surface Coating/Painting for Self-Sterilizing against Pathogens

Methods for sterilizing surfaces to control the spread of diseases using chemicals in liquid form need to be used frequently. These are suitable only for small-scale applications. For large-area applications, surface coatings are preferred. However, their cost, duration, and maintenance requirements make them inconvenient to use for large-area applications. In view of this, self-sterilizing, long-lasting and maintenance-free methods/techniques for disinfection are in demand to control the spread of viral diseases like COVID 19. The progress and prospects in nanoscience today have been made possible with nanoparticle engineered photocatalytic paints and will be a roadmap to self-sterilizing against the spread of communicable diseases. Recent developments in this field of science and technology are reported and discussed in the following sections.

#### 3.1. Self Sterilizing of Pathogens with Photocatalytic Disinfection: Principle and Working

The phenomenon of photocatalysis with semiconducting materials has been known for a long time and its principle is well explained in the literature. When a semiconductor is bombarded with light of a compatible wavelength (energy equal to or greater than

the semiconductor's band gap), the light is absorbed, resulting in the formation of an electron and hole pair.

The excited electron-hole pair generated in the semiconducting material then travels toward the semiconductor's surface. At the same moment, oxidation and reduction reactions on the semiconductor's surface take place. Figure 4 shows this conceptually. In the CB, electrons react with oxygen ( $O_2$ ) to create superoxide and hydroperoxide radicals. During the photocatalysis process, reactive oxygen species (ROS) are produced; further, it can induce leakage of minerals, genetic material and protein, and therefore result in cell death and a reduction in microbial load [84].

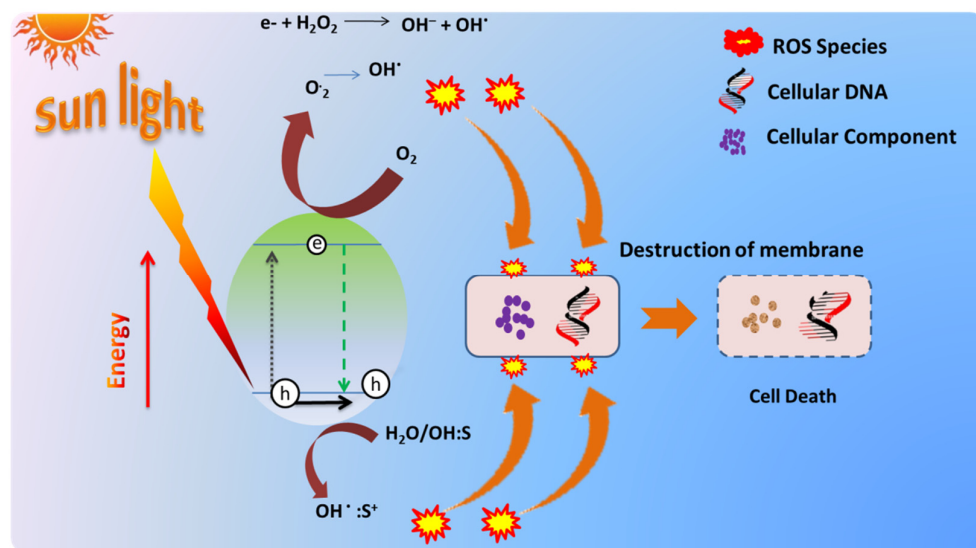


**Figure 4.** The fundamental mechanism of photocatalysis on a semiconductor particle surface for microbial treatment.

In this process, ROS oxidizes the proteins, lipids, bacteria, and enzymatic systems of viruses, resulting in the loss of their ability to reproduce due to either damage to other key proteins or damaged membranes, such as the spike protein of SARS-CoV-2. Once the pathogen comes into contact with the photocatalytic surface, it oxidizes key proteins and inactivation takes place, due to the production of ROS [85,86].

The contaminants (viral proteins, genome, and envelope) in the indoor air are photodegraded by the photocatalytic material in general. Antimicrobial photocatalysis can be utilized to disinfect air, water and surfaces [87–89].

Adsorption-desorption, electron-hole pair generation, electron pair recombination and chemical reaction are all phases in the activation of photocatalytic nanoparticles present in the nanocomposite. Figure 5 shows the hypothesized mechanism for nanocomposite photocatalytic antibacterial activity.

It has a number of benefits; for example it is a low-cost, easy-to-use, low-maintenance method that allows simultaneous disinfection of a variety of pathogens such as bacteria and viruses.

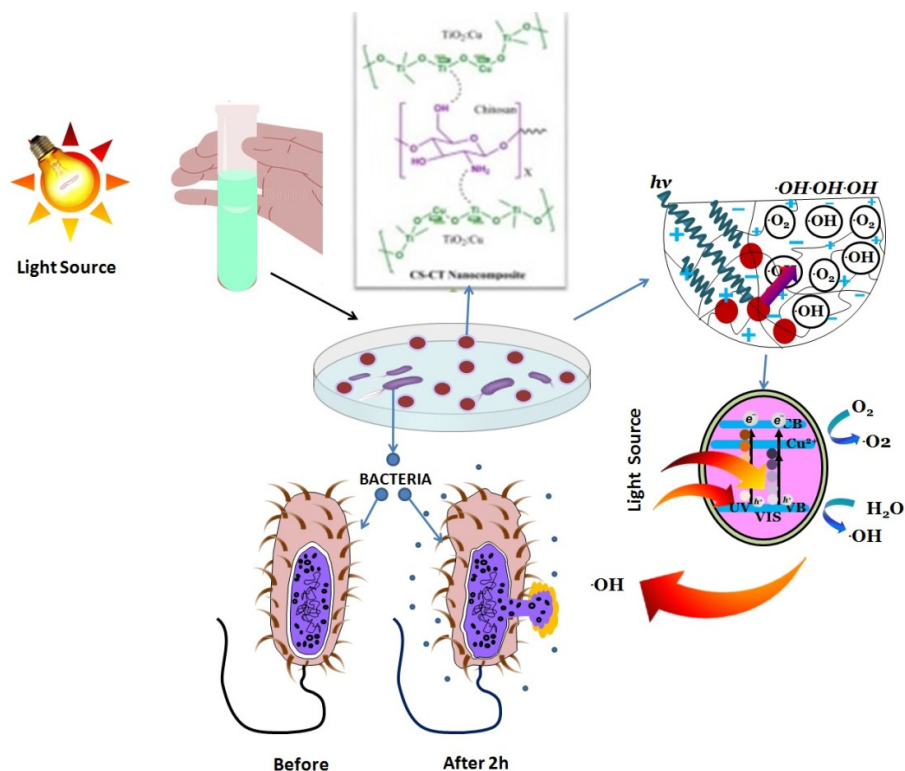


**Figure 5.** A possible mechanism for photocatalytic antibacterial activity resulting from light stimulation of nanocomposites [90]. Reproduced from Raut et al.

### 3.2. Engineering of Nanoparticles with Dopants for Visible Light Photocatalytic Disinfection

Various single-semiconductor materials have been examined as a solution for the photocatalytic breakdown of pollutants, including  $\text{TiO}_2$ ,  $\text{Cu}_2\text{O}$ ,  $\text{ZnO}$ ,  $\text{SnO}_2$ ,  $\text{WO}_3$ ,  $\text{Fe}_2\text{O}_3$  and  $\text{CdS}$ . Due to its activation by UV light, long-term stability and non-toxicity,  $\text{TiO}_2$  and its hybrid compounds have been researched as viable photocatalytic materials for the destruction of pollutants and viruses, as well as the conversion of  $\text{CO}_2$  and hydrogen production through water splitting [91].

$\text{TiO}_2$  in the anatase crystal phase has a bandgap of 3.2 eV and absorbs UV light with wavelengths shorter than 400 nm, indicating photocatalytic activity. However, due to the wide bandgap and fast recombination of the electron–hole pair, the usage of  $\text{TiO}_2$  semiconductors as photocatalysts still has a drawback of low absorption and efficiency. When considering indoor use, the use of visible light, lower in energy than UV light is unavoidable. UV light, on the other hand, accounts for less than 10% of solar energy, whereas visible light accounts for roughly 48% [92].

Several methods have been investigated to solve these problems, including: (i) modifying the surface area, crystallinity, and porosity of  $\text{TiO}_2$  particles; (ii) doping and coating the surface with metals (Se, Cu, Pd, Cd, and Pt); and (iii) combining p-type materials with  $\text{TiO}_2$  particles to form a p–n heterojunction semiconductor. Combining  $\text{TiO}_2$  with a semiconductor with a tiny bandgap, such as  $\text{CdS}$ ,  $\text{Cu}_x\text{O}$ ,  $\text{PbS}$ , or  $\text{CuS}$ , is a viable technique for boosting visible-light activity or permitting photogenerated electrons to be transported from the conduction band to other semiconductors to prevent electron–hole pair recombination. Copper is recognized as good for mixing with other stable materials since it is highly oxidative and adaptable. Furthermore, past research has shown that copper may be easily produced alone or in combination with other compounds, and that it is stable [93,94].

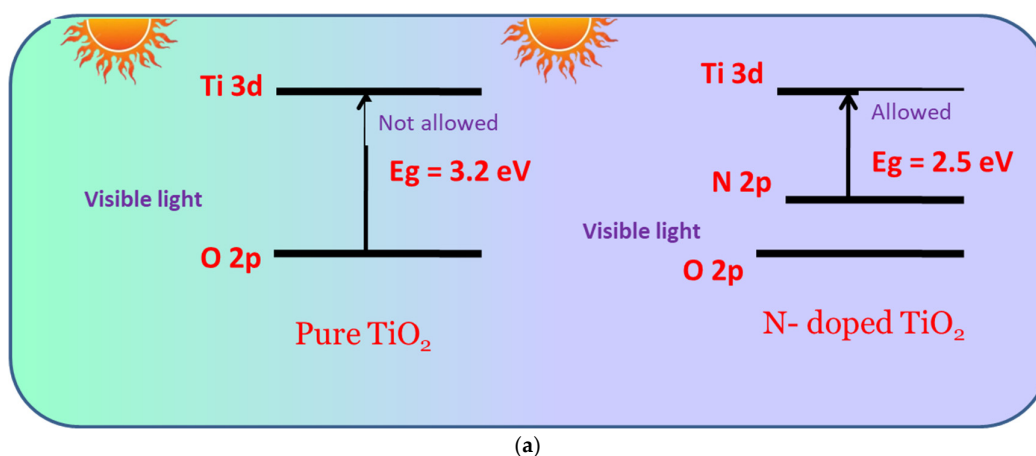
As a result, various efforts have been undertaken to improve the photocatalytic efficacy of  $\text{TiO}_2$  using a copper-based material as a p-type semiconductor, such as copper

oxide or copper sulfide. Because photocatalysts made of  $\text{TiO}_2$  can participate in a variety of reactions, including breakdown and reduction, the crystal structure and bandgap must be tailored to maximize performance.  $\text{Cu-TiO}_2$  nanorods outperformed pure  $\text{TiO}_2$  photocatalytically in both visible and ultraviolet light.

The majority of the time, thermal plasma treatment is used to prepare  $\text{TiO}_2$  and combine it with a copper-based semiconductor. Methods include hydrothermal, sol-gel and combustion. Most of the methods discussed above have the drawback of requiring a significant amount of time and energy, as well as a variety of additives and templates for synthesis. A microwave synthesis approach was proposed as a good way to avoid wasting time and energy in this way with quick and uniform heating, especially in the case of a synthesis method using dielectrics such as water.

Furthermore, it is known that lowering the Gibbs energy of activation and boosting hydrolysis can promote the reaction of transition metal ions, with which it is difficult to create a complex under usual conditions [95–97]. The bandgap of  $\text{TiO}_2$  semiconductor has been reduced from 3.2 eV to 2.5 eV due to nitrogen doping, making it sensitive to visible light, as shown in Figure 6,b.

Similarly, other dopants, such as  $\text{Cu}_2\text{O}$ ,  $\text{C}_3\text{N}_4$ ,  $\text{CdS}$  in  $\text{TiO}_2$ , Au, Ag, N, Pt, etc., are used for photocatalytic disinfections. Accordingly, the band gap will be changed. [98–105].



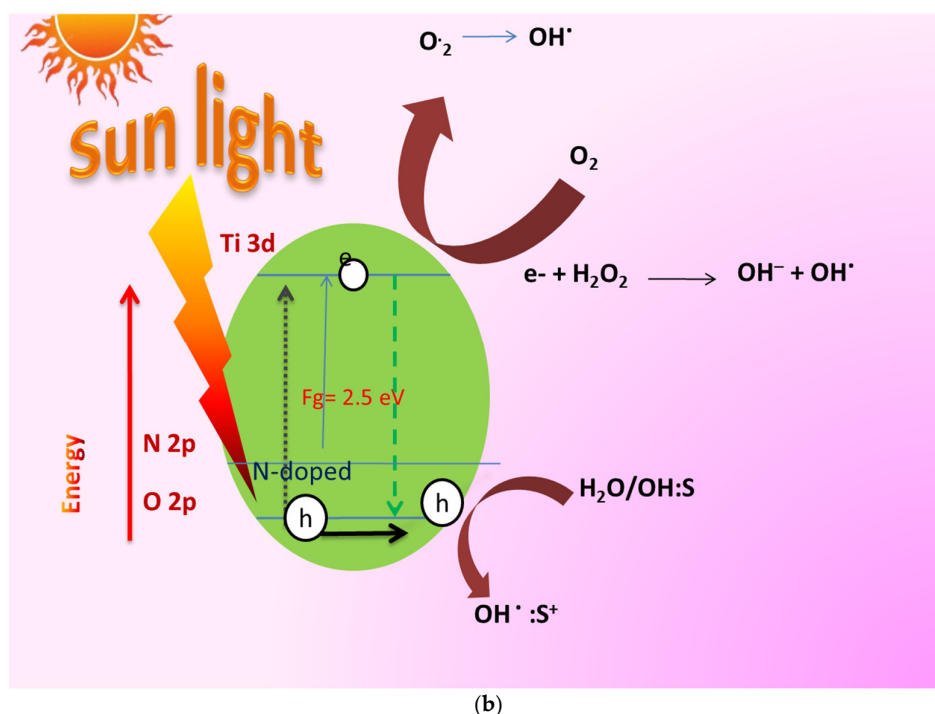


**Figure 6.** Schematic representation of the energy level diagrams of bare TiO<sub>2</sub> and N-doped TiO<sub>2</sub> (a) and reaction mechanism of the degradation of organic dyes/pathogens in the presence of N-doped TiO<sub>2</sub>. (b).

#### 4. Synthesis of TiO<sub>2</sub> Engineered Nanoparticles for Visible Light Photocatalytic Disinfections

##### 4.1. TiO<sub>2</sub> Nanoparticles: A Potential Candidate for Photocatalytic Paints

Nanosized TiO<sub>2</sub> has been studied extensively for decades due to its unusual photocatalytic characteristics. The photocatalytic inactivation of hazardous microbes is gaining popularity as one of the many environmental applications enabled by such a nanoscale material. Many researchers have described the antibacterial activity of commercially available TiO<sub>2</sub> NPs in the last few years. Innovative approaches to the production of unique TiO<sub>2</sub>-based nanomaterials, specifically tailored for photocatalytically assisted inactivation of bacteria and viruses, have recently been published. Such approaches vary in terms of the degree of complexity and production costs, but they allow access to photocatalytic TiO<sub>2</sub>-based nanomaterials with purposefully selected physical-chemical properties, such as controlled dimensions and geometry, and thus size-dependent characteristics, engineered surface chemistry, enhanced colloidal stability even under different ionic strength conditions, and biocompatibility, which is particularly useful in the fields of health-care and food preservation. A variety of synthetic routes for the preparation of nanosized TiO<sub>2</sub> with photocatalytic antimicrobial properties have been proposed in the literature; here, we focus on sol-gel and phytosynthesis, as they have been regarded as promising techniques for the large-scale production of TiO<sub>2</sub> NPs, owing to their user- and environment-friendly procedures and low costs. However, for the purpose of brevity, we will only present a tiny sample of the many examples described in the literature and we will refer readers to more detailed articles, particularly in the fields of health-care and food preservation [106].

##### 4.2. Phyto Synthesis of TiO<sub>2</sub> Nanoparticles

Researchers have currently focused their attention on the synthesis of nanoparticles using green methods, one of which is the route of biosynthesis. It mainly consists of mi-

crobial synthesis and phytosynthesis. In the present review, we have focused on the preparation of nanoparticles by the method of phytosynthesis. The plant species of lemongrass, *Annonasquamosa*, *Leechaikottaikeerai* (*Pisoniagrandis*), *Andrographispaniculata* and *Azadirachta indica* have been considered for phytosynthesis of  $\text{TiO}_2$  nanoparticles, as these are locally available in plenty and will help to produce nanoparticles on a large scale required for their commercial applications [107–111].

We present a green method for making  $\text{TiO}_2$  and  $\text{ZnO}$  nanoparticles that uses lemongrass extract as a capping agent to keep the size of the nanoparticles under control. We discovered that the extracts of phytochemical content aided in the creation of nanoparticles, as evidenced by morphologic data gathered from microscopy pictures. The nanoparticles' physicochemical properties are comparable to those of nanoparticles generated using standard methods. Finally, the anticorrosive, antibacterial, and self-cleaning properties of  $\text{TiO}_2$  and  $\text{ZnO}$  nanoparticles in paints were studied to establish their efficacy.

To remove contaminants, lemongrass leaves were trimmed, rinsed and dried before being hand-crushed. A hundred grams of biomass were placed in cotton bags and solvent-extracted for 6 h with 500 mL of distilled water. After that, the lemongrass extract was stored at 4 °C. Then, in a 250 mL beaker, 100 mL of this extract was combined with 20 mL of the precursor  $\text{C}_{12}\text{H}_{28}\text{O}_4\text{Ti}$  by dropwise addition. The solution was placed in an ultrasonic processor for around 30 min to react. The nanoparticles were rinsed with distilled water and ethanol reagent grade before being recovered by centrifugation at 5000 r/min for 30 min, with the operation repeated multiple times to eliminate any unreacted precursor. The anatase phase of  $\text{TiO}_2$  nanoparticles was obtained by calcining them at 550 °C for 3 h [107].

Roopan et al. have studied the phytosynthesis of rutile  $\text{TiO}_2$  nanoparticles using agricultural waste, such as aqueous extract of *Annona squamosa* fruit peels, at a lower temperature for the first time with the rapid production of nanoparticles. The UV–Vis spectrophotometer results were promising, with a surface plasmon resonance occurring at 284 nm, indicating its applications for photocatalytic disinfection [108]. The phytosynthesis of  $\text{TiO}_2$  nanoparticles using the extract of *Leechaikottaikeerai* (*Pisoniagrandis*) was achieved for the first time by Vembu et al., and confirmed their formation, shape, crystallinity, and an average size of 34 nm. They also studied the antimicrobial and cytotoxic activities of these nanoparticles [109]. Rajeshkumar et al. have reported phytosynthesis of titanium dioxide ( $\text{TiO}_2$ ) nanoparticles using the king of bitter herbal plant *Andrographispaniculata*. This method is eco-friendly, produces nanoparticles at a low cost, and can provide high-quantity industrial production using biodegradable and reusable natural resources [110]. The plant extracts of *Azadirachta indica* were also used by Thakur et al. as the best local source material for the phytosynthesis of  $\text{TiO}_2$  nanoparticles. This is a simple, inexpensive and eco-friendly process which reduces the use of toxic chemicals. These nanoparticles exhibited an average size of about 22.97 nm and a broad spectrum of antimicrobial activity against a vast range of pathogens [111].

#### 4.3. Synthesis of Nitrogen Doped $\text{TiO}_2$ Nanoparticles by Sol-Gel Technique

The sol–gel technique was used to create  $\text{TiO}_2$ -based photocatalysts with different dopants to make them sensitive for visible light. In this section, we have briefed the attempts of different groups of researchers to dope  $\text{TiO}_2$  nanoparticles with nitrogen by employing the solgel technique.

Cheng et al. have used tetrabutyl titanate as the basic compound of titanium. To make  $\text{Ti}(\text{OBu})_4\text{--C}_2\text{H}_5\text{OH}$  solution, 10 mL of tetrabutyl titanate was dissolved in 40 mL of anhydrous ethanol in a usual procedure. Meanwhile, 12 mL of dilute nitric acid (1:5, volume ratio of nitric acid to deionized water) and a small amount of ammonium chloride were added to another 10 mL of anhydrous ethanol to make a  $\text{C}_2\text{H}_5\text{OH--HNO}_3\text{--water}$  solution. To carry out hydrolysis, the  $\text{C}_2\text{H}_5\text{OH--HNO}_3$  solution was gently added dropwise to the  $\text{Ti}(\text{OBu})_4\text{--C}_2\text{H}_5\text{OH}$  solution while vigorously stirring. After that, the re-

sulting yellowish, transparent sol was aged for 6 h after being stirred constantly for 2 h. The resulting yellowish, clear sol was next dried for 36 h at 80 °C in an oven and then calcined for 4 h at a specific temperature, with a heating rate of 3 °C per minute [112].

Than et al. synthesized N-doped anatase TiO<sub>2</sub> nanoparticles (N-TiO<sub>2</sub> NPs) from titanium chloride (TiCl<sub>4</sub>) and ammonia (NH<sub>3</sub>) via the sol-gel method. The high visible light activity of the N-TiO<sub>2</sub> nanomaterials was recognized in the interstitial nitrogen atoms inside the TiO<sub>2</sub> lattice units. These findings could provide a practical pathway capable of large-scale production of a visible-light-activated N-TiO<sub>2</sub> photocatalyst. The interstitial nitrogen atoms within the TiO<sub>2</sub> lattice units played an important role in generating intermediate energy levels and narrowing the bandgap, thereby enhancing the VLA of the materials [113]. Reda et al. synthesized Cu and N-doped TiO<sub>2</sub> photocatalysts using titanium (IV) isopropoxide via a microwave-assisted sol-gel method. For N doping, ammonium nitrate was utilized as a raw source. The doped TiO<sub>2</sub> samples showed a higher surface area (253–383 m<sup>2</sup>/g) than that of the pure one (151 m<sup>2</sup>/g) and exhibited better light-harvesting in both visible and UV light regions [114]. The nitrogen-doped titanium oxide was successfully synthesized through an EDTA modified sol-gel process by Nassoko et al. Here EDTA is used as source of nitrogen for doping. The results showed that through the simple sol-gel process, nitrogen can be incorporated into the crystal lattice of TiO<sub>2</sub>, leading to its response to visible light [115]. N-doped titania is synthesized using the various nitrogen sources such as, triethylamine, N,N,N',N'-tetramethylethane-1,2-diamine, ethyldiamine, 1,2-phenylenediamine, propanolamine, and propylenediamine and TTIP was used as a TiO<sub>2</sub> source by Mehdizadeh et al. The bandgap of N/TiO<sub>2</sub> has changed from 3.38 eV (pure TiO<sub>2</sub>) to 3.26 eV for N/TiO<sub>2</sub>:2.0. It could limit the band gap of titania and its absorption extends to the visible light region; moreover, it might increase the separation efficiency of the photoinduced electron and hole [116].

#### 4.4. Synthesis of CNTs Doped TiO<sub>2</sub> Nanoparticles by Sol-Gel Technique

A sol-gel technique was also used to make CNT-doped TiO<sub>2</sub> nanoparticles by different groups of researchers to make the paint of photocatalytic disinfection sensitive to visible light.

Akhavan et al. used Titanium (IV) n-butoxide as basic chemical compound of titanium. First, 2.3 mL Titanium (IV) n-butoxide was dissolved in 23 mL ethanol. The solution was then agitated for 30 min to make it homogenous. Another solution was made with 2 mL of nitric acid and the desired amount of CNTs. Drop by drop, the CNT–nitric acid solution was added to the alkoxide–ethanol solution, and the mixture was agitated for 2 h. The molar ratio of H<sub>2</sub>O to titanium n-butoxide in the final solution was 2.7:1. The solution was left at room temperature for 24 h to age. Dip-coating was used to deposit CNT-doped TiO<sub>2</sub> films on glass substrates. The substrate was dragged at a steady speed of 1 mm/s after being soaked in the solution for roughly 1 min. After drying the samples at room temperature for 24 h, they were heated in air for 1 h at 100 °C. Furthermore, parts of the CNT-doped TiO<sub>2</sub> thin films were heat treated in air for 1 h at 450 °C [117].

Shafei et al. synthesized TiO<sub>2</sub>-10wt. % CNT nanocomposite powder doped with 1 at.% Cu using this sol-gel method. Band gap energy decreased from 3.2 to 3.05 eV by addition of CNTs to the TiO<sub>2</sub> and decrease further to 2.85 eV by both the addition of CNT and Cu doping to TiO<sub>2</sub> [118]. Mohammad et al. synthesized single-walled carbon nanotubes (SWCNTs) and multiwalled carbon nanotubes (MWCNTs), which were chemically treated with sulfuric acid (H<sub>2</sub>SO<sub>4</sub>) and nitric acid (HNO<sub>3</sub>) in a ratio (3:1). These carbon nanotubes (CNTs) have been coated with Ag-doped TiO<sub>2</sub> nanoparticles (NPs) using the sol-gel method. The band gap value of 3.6 eV was obtained from raw MWCNTs, while the corresponding value of the raw-SWCNT sample was 2.94 eV. The addition of TiO<sub>2</sub>/Ag NPs leads to a decrease in the band gap, 2.69 eV for MWCNTs-TiO<sub>2</sub>/Ag and 2.6 eV for SWCNTs-TiO<sub>2</sub>/Ag [119]. Carbon-doped titanium dioxide (TiO<sub>2</sub>) coating on multiwalled carbon nanotubes (MWCNTs) was prepared by oxidation of ti-



tanium carbide (TiC) coated MWCNTs by Cong et al. MWCNTs, which may act as a supporting, absorbent, photo-generated transfer station and carbon-doping source play key roles in narrowing the band gap of TiO<sub>2</sub> [120].

## 5. Smart Paint Formulations with Nanostructured Additives for Their Photocatalytic Activities

### 5.1. Updates of Photocatalytic Paints Studied for Pathogenic Disinfections

With the developments in the engineering of nanoparticles with dopants for visible light photocatalytic disinfection, the next step is to use these findings for large-area applications specifically for controlling the spread of communicable diseases such as COVID-19. In this regard, few research groups including our group have attempted smart paint formulations with nanostructured additives for their photocatalytic activities with an intention to disinfect the pathogens. The survey of such data is of recent origin and the first of its kind in the literature reported in Table 4.

**Table 4.** The Summary of Photocatalytic Paints used in pathogenic disinfections.

Sr. No.	Paint Used	Material	Dopant Used	Pathogenic Disinfection			Source of Light	Band Gap Energy & Particle Size	References
				Microbial	Fungal	Viral			
1	KEIM Ecosil ME, Titanium FA, Photo Silicate and Silicate D	TiO <sub>2</sub>	-	-	<i>Trichoderma viride</i> , <i>Aspergillus niger</i> , <i>Coonemeria crustacea</i> , <i>Eurotium herbariorum</i> , and <i>Dactylomyces</i> sp	-	UV light	-	[121]
2	Acrylic paint	TiO <sub>2</sub>	-	-	<i>Monascus ruber</i> , <i>Metals: copper</i> (Cu), <i>silver</i> (Ag), <i>manganese</i> (Mn)	-	UV light	945 nm	[122]
3	Photocatalytic paint	TiO <sub>2</sub>	Non-metals: fluorine (F), calcium (Ca), phosphorus (P)	<i>Escherichia coli</i> , <i>methicillin-resistant Staphylococcus aureus</i> , <i>Pseudomonas aeruginosa</i> , <i>Bacillus subtilis</i> , <i>Legionella pneumophila</i> , <i>Staphylococcus aureus</i> , <i>Streptococcus mutans</i> , <i>T2 bacteriophage</i> , <i>H1N1</i> , <i>HCoV NL63</i> , <i>vesicular stomatitis virus</i> , <i>bovine coronavirus</i> .	-	-	UV-Visible light	3.5 eV 20–30 nm	[123]
4	Acrylic paint	TiO <sub>2</sub> /ZnO	-	<i>Escherichia coli</i> , <i>Pseudomonas aeruginosa</i> , and <i>Staphylococcus aureus</i> , <i>Penicillium</i>	-	-	UV light	-	[124]

				<i>chrysogenum</i> and <i>Aspergillus niger</i>					
5	Photocatalytic paint	TiO <sub>2</sub>	-	<i>Escherichia coli</i>	-	-	UV-light	3.2 eV	[125]
6	Photocatalytic paint	TiO <sub>2</sub>	Carbon	-	<i>Aspergillus niger</i>	-	UV & Visible	-	[126]
7	Photocatalytic paint	TiO <sub>2</sub>	Carbon	<i>A. baumannii</i> and <i>S. flexneri</i>	-	-	UV & Visible	-	[127]
8	Photocatalytic paint	TiO <sub>2</sub>	-	<i>E. coli</i>	<i>C. parapsilosis</i>	MS2	UV light	-	[128]
9	Photocatalytic paint	TiO <sub>2</sub>	-	-		SARS-CoV-2	UV light	-	[129]
10	Photocatalytic paint	ZnO	Ag	<i>Staphylococcus aureus</i> , <i>Pseudomonas</i> spp, <i>Salmonella</i> spp, <i>Bacillus subtilis</i> , <i>Listeria monocytogenes</i>	-	-	Visible	35 nm	[130]
11	Photocatalytic paint	TiO <sub>2</sub>	-	<i>Escherichia coli</i>	-	-	UV light	-	[131]
12	Photocatalytic paint	TiO <sub>2</sub>	-	<i>Escherichia coli</i> , methicillin-resistant <i>Staphylococcus aureus</i> , <i>Pseudomonas aeruginosa</i> , <i>Bacillus subtilis</i> , <i>Legionella pneumophila</i> , <i>Staphylococcus aureus</i> , <i>Streptococcus mutans</i>	-	H1N1, HCoV-NL63, vesicular stomatitis virus, bovine coronavirus.	UV-light	-	[132]
13	Photocatalytic paint	TiO <sub>2</sub>	Carbon nano-tubes	<i>Bacillus subtilis</i>	-	-	UV-Visible	3 eV	[133]
14	Photocatalytic paint	TiO <sub>2</sub>	Copper	<i>Escherichia coli</i> and <i>Staphylococcus aureus</i>	-	-	Visible light	2.89 eV	[134]
15	Acrylic paint	TiO <sub>2</sub>	-	<i>Escherichia coli</i> , <i>Staphylococcus aureus</i> and <i>Pseudomonas aeruginosa</i>	-	-	UV light	22.6 nm	[135]
16	Photocatalytic paint	TiO <sub>2</sub>	-	-	<i>Aspergillus niger</i> and <i>Aspergillus oryzae</i>	-	UV light	-	[136]
17	Photocatalytic paint	TiO <sub>2</sub>	-	<i>Escherichia coli</i> , <i>Staphylococcus aureus</i> , <i>Pseudomonas putida</i> and <i>Listeria innocua</i>	-		UV light	-	[137]

### 5.2. Formulation of TiO<sub>2</sub>-based Oil Paint Samples

Here we report the formulation of three types of nanostructured paints:

(a) Paint formulated with TiO<sub>2</sub> nanoparticles prepared from lemon grass leaves.

(b) Paint formulations with TiO<sub>2</sub> nanoparticles doped with nitrogen prepared by the sol-gel method.

(c) Paint formulations with TiO<sub>2</sub> nanoparticles doped with CNTs by the sol-gel method.

The paint samples were prepared using the percentile mixture of titanium dioxide nanomaterials (TiO<sub>2</sub> powder) in the white colored base oil paint with a fraction of the turpentine to obtain a homogenous mixture. The 1%, 3%, 5% and 7% paint samples were prepared and base paint control was used for the testing purpose.

For the paint mix, 30 percent distilled water and 33.4 percent resin BASF ACRONAL were utilized. The dispersing agent BASF DISPEX AA 4146 was used at 0.6 percent *w/w*, and the total amount of solids, including pigment (TiO<sub>2</sub>) and extender (CaCO<sub>3</sub> Cicarelli, >99 percent purity), was kept constant at 36 percent *w/w*. In the paints, the maximum amount of TiO<sub>2</sub> was 18 percent by weight. Other paints were also developed, with the carbon-doped TiO<sub>2</sub> quantity varying between 14 and 12 percent *w/w*. Two paints, on the other hand, were created with different amounts of CaCO<sub>3</sub>, but the percentage of carbon-doped TiO<sub>2</sub> remained constant at 18% *w/w*. Finally, various pseudo-paints were created by eliminating one of the solid matrix's components, the extender.

TiO<sub>2</sub> and CaCO<sub>3</sub> were hand milled and dried at 110°C before being used in the paints. The solids were then added to a solution of distilled water and dispersing agent, which was mixed at 300 revolutions per minute. To finish the paint, the resin was added in the last phase. Prior to the air decontamination studies, the photocatalytic coatings were subjected to visible radiation lamps. With this method, the epoxy covering the TiO<sub>2</sub> particles was damaged, permitting contact between the photocatalyst and the contaminated air [138–140].

Photocatalytic TiO<sub>2</sub>-based Nano-composite Smart Paint Formulation is summarized schematically in Figure 7.

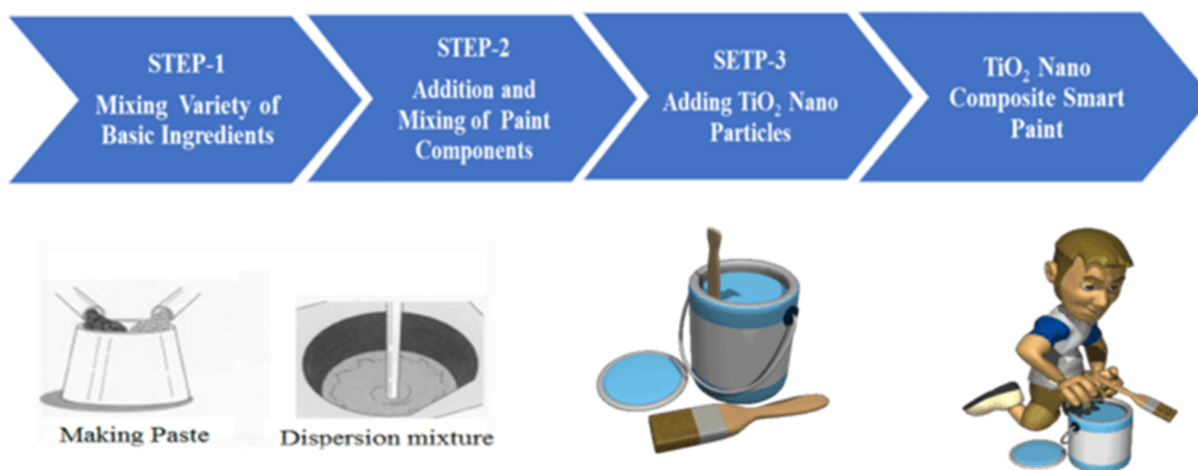


**Figure 7.** Schematics of steps involved in formulation of nanocomposite paint.

Islam et al. reported the development of photocatalytic paint based on TiO<sub>2</sub> and photopolymer resin for the degradation of organic pollutants in water. Photocatalytic paint (consisting of a mixture of TiO<sub>2</sub> and photopolymer resin) with a different weight percentage of TiO<sub>2</sub> (0–10 wt. %) was prepared in plastic Petri dishes and the degradation of organic pollutants in water was studied [141]. Laisney et al. reported the formulation of photocatalytic paints with TiO<sub>2</sub> nanoparticles coated with bio-inspired ligands for the Safer by Design. Photocatalytic paints were formulated with TiO<sub>2</sub> NPs and TiO<sub>2</sub> NPs coated with Dopa, PEG3350 and PAA. They have successfully modified the surface of a commercial photocatalytic TiO<sub>2</sub> nanopowder with bio-inspired ligands of different chemical nature (molecules and polymers) for its application in self-cleaning paint [142].

Rosset et al. reported the development of TiO<sub>2</sub>-based photocatalytic paint. TiO<sub>2</sub> NPs synthesized were incorporated into an organic matrix-based paint. The organic-based

paint was composed of acrylic, micro-sized  $\text{TiO}_2$  providing the white color (pigment), calcium carbonate particles, aluminosilicate, water and other additives. The micro-sized  $\text{TiO}_2$  particles have a mean particle size distribution (PSD) of the primary particles of 240 nm [143]. Basso et al. reported a photocatalytic effect of the addition of  $\text{TiO}_2$  to acrylic-based paint for passive toluene degradation. Photocatalytic paints were formed by adding  $\text{TiO}_2$  P25 powder to an acrylic-based paint. Photocatalytic paint samples were prepared by adding  $\text{TiO}_2$  P25 to the paint in the following proportions (dry basis): 0, 10, 15, 20 and 50 wt. %. Complete dispersion was achieved by stirring different amounts of paint and  $\text{TiO}_2$  P25 in a glass beaker, using a laboratory overhead stirrer at 300 rpm, for 20 min [144].

### 5.3. A Field Study of Photocatalytic Nanocomposite Paints for Pathogenic Disinfections

Ren et al. investigated microbial activity on the walls of two Hong Kong schools with and without photocatalytic  $\text{WOx}$  paint coatings;  $\text{WOx}$  paints were painted on the semi-outdoor and indoor walls in Tun Mun and Tin Shui Wai schools, and daily chlorine disinfection was performed after class in Tin Shui Wai School. For large-scale field experiments, a technique using the ATP biofluorescence approach was presented. On a control basis, ATP swab samples were collected once a week for three months in areas with and without the  $\text{WOx}$  paint. After that, the ATP data were processed and plotted in box plots. The median log-scale ATP values of walls with  $\text{WOx}$  paint were at least 0.5 log lower than those without  $\text{WOx}$  paint in both schools. In the long run, the  $\text{WOx}$  paint was more effective than daily chlorine disinfection at reducing microbial activity. The proposed testing technique is determined to be suitable for evaluating the long-term performance of an antimicrobial paint in large-scale field experiments by assessing its microbial activity. In both indoor and semi-outdoor conditions, the  $\text{WOx}$  paint exhibits long-term efficiency in lowering microbial activity on wall surfaces [145].

The systematic use of the ATP bioluminescence strategy was shown to be beneficial in conducting a field investigation of tracking surface microbial activity on various surfaces in a large-scale disinfection practice to evaluate its practical effectiveness. They have also provided a step-by-step guide for creating a testing strategy for evaluating an antimicrobial paint's long-term efficacy. This systematic technique can be a valuable and low-cost tool for evaluating the field performance of the large number of disinfection strategies that claim to be successful in the long term, particularly those that arose during the COVID-19 period. The findings from the two primary schools showed that the RAZE photocatalyst paint was successful in lowering microbial activity on wall surfaces in both indoor and semi-outdoor situations. In settings where low microbial activity is required, such as hospitals, schools, and kindergartens, RAZE paint has a lot of potential. To meet stricter disinfection requirements, more work is needed to improve its efficacy when alternative disinfection procedures, such as chlorine disinfection, are used. Furthermore, the differences in log-scale ATP values in the aforementioned scenario-based analysis highlighted the need for more research into the effects of disinfection strategies, such as chlorine disinfection with RAZE paint and chlorine disinfection alone, on microbial species evolution using, for example, metagenomic analysis. Such research will aid the community in better understanding how to choose more appropriate disinfection procedures to safeguard our living environment while avoiding the potential for microbial species to become stronger and more resistant [146,147].

The proposed testing protocol is suitable to evaluate the long-term performance of an antimicrobial paint by analyzing its microbial activity in large-scale field tests. The  $\text{TiO}_2$  doped paint shows long-term effectiveness in reducing microbial activity on wall surfaces in both indoor and semi-outdoor environments.

## 6. Conclusions

Based on the critical survey of the relevant literature referred in this review and our experience in fighting against communicable diseases, during the past few years, the following conclusions can be drawn:

(1) COVID-19 disease has remained persistent for longer than 24 months since December 2019, and it has affected millions of people worldwide.

(2) There remains the significant challenge of preventing infections due to the spread of the SARS-CoV2 virion as it is a bio-nanoparticle. Apart from its biological structures, the nano structural properties do change drastically with their shape and size as per the knowledge of nanoscience, and thus its eradication is still uncertain.

(3) The transmission of SARS-CoV2 viruses also takes place through contact surfaces such as doorknobs, packaging and handrails in public places. This may be responsible for many preventable and nosocomial infections.

(4) The spread of communicable diseases may be attributed to different phenomena such as the multiplication, transmission and persistence of viruses.

(5) The persistence of viruses such as SARS-CoV-2 in/on different 22 environmental matrices has been researched and presented for the first time collectively in this review. It may be noted that the spread of communicable diseases may be predominantly attributed to the phenomenon of persistence of viruses on different substrates for different durations.

(6) The existing antimicrobial cleaning technologies used in hospitals are not suitable, viable or economical to keep public places free from such infections.

(7) As an alternative to existing sterilization techniques, photocatalytic pathogen disinfectant surface coatings/paintings have been developed in recent years.

(8) Smart paint formulations with a variety of nanostructured additives for their photocatalytic pathogen disinfectant activities have been attempted in recent years, but in a very limited way. Reports on a variety of photocatalytic paints studied for their pathogen disinfection potential are reviewed and listed together for first time to make their comparison easier.

(9) The protection of public places with smart paint photocatalytic pathogenic disinfectant coatings may help to control the spread of communicable diseases such as COVID-19.

## 7. Future Suggestions

Health-care is of prime importance for humanity globally. Communicable diseases such as COVID-19 have raised a great threat due to infectious virions like SARS-CoV-2. The means to control such virions are discussed in this review. Based on the contents of the review and present needs, the following are key suggestions to build a roadmap to self-sterilizing against the spread of communicable diseases:

(1) Visible-light-sensitive nanoparticle engineered photocatalytic paints need to be formulated and tested for their pathogen disinfectant activity in field applications in public places.

(2) The durability, viability and impact on the environment of the photocatalytic paint coatings in open public places need to be studied.

(3) The economic viability of the methods of surface sterilization with conventional techniques and with the newly suggested visible-light photocatalytic disinfection of pathogens needs to be compared and the suitability of new method should be worked out.

(4) A roadmap to self-sterilizing against the spread of communicable diseases is still at a conceptual level and needs to be given more thought before its implementation on a large scale.

**Author Contributions:** Conceptualization, S.H.P.; methodology, M.M.D.; validation, R.K.S.; formal analysis, V.S.M.; investigation, S.H.P.; resources, M.M.D.; data curation, R.K.S.; writing—

original draft preparation, V.S.M. and S.H.P.; writing—review and editing, V.S.M. and S.H.P.; visualization, M.M.D.; supervision, S.H.P.; project administration, V.S.M.; funding acquisition, S.H.P. All authors have read and agreed to the published version of the manuscript.”

**Funding:** This research received no external funding

**Data Availability Statement:** Not Applicable

**Acknowledgments:** The authors are grateful to Principal C. V. Murumkar and P. C. Pingale from T.C. College, Baramati and R. K. Mudgal, Vice-Chancellor and Shimpa Shrama, Pro.Vice-Chancellor from D.Y.Patil Education Society, deemed to be university, Kolhapur for their constant encouragement and support during this work.

**Conflicts of Interest:** The authors declare no conflict of interest.

## References

1. Pawar, S.H. *Progress and Prospects in Nanoscience Today*, Nova Science Publishers: Hauppauge, NY, USA, 2020.
2. Sawant, D.V.; Desai, M.M.; Patil, R.S.; Pawar, S.H. Evolution of nanotech assisted PCR diagnosis of Mycobacterium tuberculosis and its assessment with conventional methods. *Int. J. Pharm. Pharm. Sci.* **2018**, *10*, 133–137.
3. Sawant, D.V.; Bohara, R.A.; Patil, R.S.; Pawar, S.H. Detection of Mycobacterium tuberculosis from pulmonary sputum sample using SPION mediated DNA extraction method. *Res. J. Life Sci. Bioinform. Pharm. Chem. Sci.* **2018**, *4*, 4.
4. Deepak, V.S. Shivaji, H.P. Studies on gold nanobiosensor for early diagnosis of Mycobacterium tuberculosis. *Int. J. Pharm. Biol. Sci.* **2019**, *9*, 77–82.
5. Armelin, E. Liesa, F. Estrany, F. Marine paint formulations: Conducting polymers as anticorrosive additives, *Prog. Org. Coatings*, **2007**, *59* (1), 46–52
6. Tornero, A.C.F.; Blasco, M.G.; Azqueta, M.C. Antimicrobial ecological waterborne paint based on novel hybrid nanoparticles of zinc oxide partially coated with silver. *Prog. Org. Coat.* **2018**, *121*, 130–141.
7. Yazid, S.A.; Mohd, Z.; Mohamad, J. Effect of titanium (IV) isopropoxide molarity on the crystallinity and photocatalytic activity of titanium dioxide thin film deposited via green sol-gel route. *J. Mater. Res. Technol.* **2018**, *8*, 1434–1439.
8. Wang, L.; Hu, C.; Shao, L. The antimicrobial activity of nanoparticles: Present situation and prospects for the future. *Int. J. Nanomed.* **2017**, *12*, 1227–1249.
9. Abbas, M.; Iftikhar, H.; Malik, M.H.; Nazir, A. Surface Coatings of TiO<sub>2</sub> Nanoparticles onto the Designed Fabrics for Enhanced Self-Cleaning Properties. *Coatings* **2018**, *8*, 35.
10. Mo, C.; Zhang, Y.; Wang, F.; Mo, Q. A Simple Process for Fabricating Organic/TiO<sub>2</sub> Super-Hydrophobic and Anti-Corrosion Coating. *Int. J. Electrochem. Sci.* **2015**, *10*, 7380–7391.
11. Rabajczyk, A.; Zielecka, M.; Klapsa, W.; Dziechciarz, A. Self-Cleaning Coatings and Surfaces of Modern Building Materials for the Removal of Some Air Pollutants. *Materials* **2021**, *14*, 2161.
12. Diamanti, M.V.; Del Curto, B.; Ormellese, M.; Pedferri, M.P. Photocatalytic and self-cleaning activity of colored mortars containing TiO<sub>2</sub>, *Construction and Building Materials*, **2013**, *46*, 167–174
13. Amorim, S.M.; Suave, J.; Andrade, L.; Mendes, A.; José, H.J.; Moreira, R.F.P.M. Towards an efficient and durable self-cleaning acrylic paint containing mesoporous TiO<sub>2</sub> microspheres. *Prog. Org. Coat.* **2018**, *118*, 48–56.
14. Ling, Y.; Zhang, C.; Wu, J.; Xu, W.; Qi, Y.; He, P. Enhanced photocatalytic activity of TiO<sub>2</sub> by micrometer-scale flower-like morphology for gaseous elemental mercury removal. *Catal. Commun.* **2018**, *116*, 91–95.
15. Song, H.; Cheng, K.; Guo, H.; Wang, F.; Wang, J.; Zhu, N. Effect of ethylene glycol concentration on the morphology and catalytic properties of TiO<sub>2</sub> nanotubes. *Catal. Commun.* **2017**, *97*, 23–26.
16. Scalarone, D.; Lazzari, M.; Chiantore, O. Acrylic protective coatings modified with titanium dioxide nanoparticles: Comparative study of stability under irradiation. *Polym. Degrad. Stab.* **2019**, *97*, 2136–2142.
17. Lan, K.; Wang, R.; Zhang, W.; Zhao, Z.; Elzatahry, A.; Zhang, X.; Liu, Y.; Al-Dhayan, D.; Xia, Y.; Zhao, D. Mesoporous TiO<sub>2</sub> Microspheres with Precisely Controlled Crystallites and Architectures. *Chem* **2018**, *4*, 1–15.
18. Zhao, J.; Liao, C.; Liu, J.; Shen, X.; Tong, H. Development of mesoporous titanium dioxide hybrid poly (vinylidene fluoride) ultrafiltration membranes with photocatalytic properties. *J. Appl. Polym. Sci.* **2016**, *133*, 43427.
19. Hochmannova, L.; Vytrasova, J. Photocatalytic and antimicrobial effects of interior paints. *Prog. Org. Coat.* **2010**, *67*, 1–5.
20. Auvinen, J.; Wirtanen, L. The influence of photocatalytic interior paints on indoor air quality. *Atmos. Environ.* **2008**, *42*, 4101–4112.
21. Rincon, A. & Pulgarin, C, Photocatalytical inactivation of E. coli; effect of (continuous– intermittent) light intensity and of (suspended–fixed) TiO<sub>2</sub> concentration, *Applied Catalysis B: Environmental*, **2003**, *44*, 263–284
22. Gaylarde, C.C.; Morton, L.H.G.; Loh, K.; Shirakawa, M.A. Biodeterioration of external architectural paint films—A review. *Int. Biodeterior. Biodegrad.* **2011**, *65*, 1189–1198.
23. Pittol, M.; Tomacheski, D.; Simões, D.N.; Ribeiro, V.F. RMC Santana, Antimicrobial performance of thermoplastic elastomers containing zinc pyrithione and silver nanoparticles. *Mater. Res.* **2017**, *20*, 1266–1273.

24. Kwon, J.; Choi, K.; Schreck, M.; Liu, T.; Tervoort, E.; Niederberger, M. Gas-Phase Nitrogen Doping of Monolithic TiO<sub>2</sub> Nanoparticle-Based Aerogels for Efficient Visible Light-Driven Photocatalytic H<sub>2</sub> Production. *ACS Appl. Mater. Interfaces*. **2021**, *13*, 53691–53701.
25. Darade, M.M.; Sawant, D.V.; Sharma, R.K.; Pawar, S.H. An Additional Approach to Control the Spread of COVID-19 with Photocatalytic Disinfection by Nanocomposite Painting. *IJSER*, **2021**, *12*. <https://www.ijser.org/research-paper-publishing-october-2021.aspx> (accessed on 5 March 2022)
26. Stephanie, J. Dancer, Controlling Hospital-Acquired Infection: Focus on the Role of the Environment and New Technologies for Decontamination. *Clin. Microbiol. Rev.* **2014**, *27*, 665–690.
27. Zhang, R.; Li, Y.; Zhang, A.L.; Wang, Y.; Molina, M.J. Identifying airborne transmission as the dominant route for the spread of COVID-19. *Proc Natl Acad Sci. USA* **2020**, *117*, 202009637.
28. Zhang R, Li Y, Zhang AL, Wang Y, Molina MJ, Identifying airborne transmission as the dominant route for the spread of COVID-19, *Proc Natl Acad Sci.*, **2020**, *117*(26), 202009637
29. Stadnytskyi, V.; Bax, C.E.; Bax, A.; Anfinrud, P. The airborne lifetime of small speech droplets and their potential importance in SARS-CoV-2 transmission. *Proc. Natl. Acad. Sci. USA*, **2020**, *117*, 11875–11877.
30. Morawska, L.; Milton, D.K. It is time to address airborne transmission of COVID-19. *Clin. Infect. Dis.* **2020**, *71*, 2311–2313. <https://doi.org/10.1093/cid/ciaa939/5867798>.
31. Colson, P.; la Scola, B.; Levasseur, A.; Caetano-Anollés, G.; Raoult, D. Mimivirus: Leading the way in the discovery of giant viruses of amoebae, *Nat. Rev. Microbiol.* **2017**, *15*, 243–254.
32. Ng, T.F.F. Preservation of viral genomes in 700-y-old caribou feces from a subarctic ice patch. *Proc. Natl. Acad. Sci. USA*. **2014**, *111*, 16842–16847.
33. Malone, B.; Urakova, N.; Snijder, E.; Campbe, E. Structures and functions of coronavirus replication–transcription complexes and their relevance for SARS-CoV-2 drug design. *Nat. Rev. Mol. Cell Biol.* **2022**, *23*, 21.
34. Song, Z.; Xu, Y.; Bao, L.; Zhang, L.; Yu, P.; Qu, Y.; Zhu, H.; Zhao, W.; Han, Y.; Qin, C. From SARS to MERS, Thrusting Coronaviruses into the Spotlight. *Viruses*. **2019**, *11*, 59.
35. Ward, P. ‘COVID-19/SARS-CoV-2 Pandemic’. Faculty of Pharmaceutical Medicine Blog. 6 April 2020. Available online: <https://www.fpm.org.uk/blog/covid-19-sars-cov-2-pandemic/> (accessed on 4 Dec. 2021)
36. Moelling, K.; Broecker, F. Viruses and evolution—viruses first? A personal perspective. *Front. Microbiol.* **2019**, *10*, 523–523.
37. Retroviruses. In *Overview of Reverse Transcription*; Coffin, J.M., Hughes, S.H., Varmus, H.E., Eds.; Cold Spring Harbor (NY) Laboratory Press: 1997. <https://www.ncbi.nlm.nih.gov/books/NBK19376/>
38. Rakowska, P.; D.; Tiddia, M.; Faruqi, N.; Bankier, C.; Pei, Y.; Andrew; Pollard, J.; Zhang, J.; Ian; Gilmore, S. Antiviral surfaces and coatings and their mechanisms of action. *Commun. Mater.* **2021**, *2*, 53. <https://doi.org/10.1038/s43246-021-00153-y>.
39. Cui, J.; Li, F.; Shi, Z.L. Origin and evolution of pathogenic corona viruses. *Nat. Rev. Microbiol.*, **2019**, *17*, 181–192.
40. Tekes, G.; Thiel, H.-J. Feline Corona viruses: Pathogenesis of Feline Infectious Peritonitis. *Adv. Virus Res.* **2016**, *96*, 193–218.
41. Pica, N.; Bouvier, N.M. Environmental factors affecting the transmission of respiratory viruses. *Curr. Opin. Virol.* **2012**, *2*, 90–95.
42. Zhou, L.; Samuel; Ayeh, K.; Chidambaram, V.; Petros; Karakousis, C. Modes of transmission of SARS-CoV-2 and evidence for preventive behavioral interventions. *BMC Infect. Dis.* **2021**, *21*, 496.
43. Meselson, M. Droplets and aerosols in the transmission of SARS-CoV-2. *N. Eng. J. Med.* **2020**, *382*, 2063–2063.
44. Weber, T.P.; Stilianakis, N.I. Inactivation of influenza A viruses in the environment and modes of transmission: A critical review, *J. Infect.* **2008**, *57*, 361–373.
45. Kambhampati, A.; Koopmans, M.; Lopman, B.A. Burden of norovirus in healthcare facilities and strategies for outbreak control, *J. Hosp. Infect.* **2015**, *89*, 296–301.
46. Wolfel, R.; Corman, V.M.; Guggemos, W.; Seilmaier, M.; Zange, S.; Muller, M.A.; Niemeyer, D.; Jones, T.C.; Vollmar, P.; Rothe, C. Virological assessment of hospitalized patients with COVID-2019, *Nature*, **2020**, *581*, 465–469
47. Firquet, S. Survival of enveloped and non-enveloped viruses on inanimate surfaces. *Microbes Environ.* **2015**, *30*, 140–144.
48. Desimmie, B.A.; Raru, Y.Y.; Awadh, H.M.; He, P.; Teka, S.; Willenburg, K.S. Insights into SARS-CoV-2 Persistence and Its Relevance. *Viruses*. **2021**, *13*, 1025.
49. Lai, M.Y.Y.; Cheng, P.K.C.; Lim, W.W.L. Survival of severe acute respiratory syndrome corona virus, *Clin. Infect. Dis.* **2005**, *41*, e67–e71.
50. Chattopadhyay, D.; Chattopadhyay, S.; Lyon, W.G.; Wilson, J.T. Effect of surfactants on the survival and sorption of viruses, *Environ. Sci. Technol.* **2002**, *36*, 4017–4024.
51. Vasickova, P.; Pavlik, I.; Verani, M.; Carducci, A. Issues concerning survival of viruses on surfaces, *Food Environ. Virol.* **2010**, *2*, 24–34.
52. Cai, J.; Sun, W.; Huang, J.; Gamber, M.; Wu, J.; He, G. Indirect virus transmission in cluster of COVID-19 cases, Wenzhou, China, *Emerg. Infect. Dis.* **2020**, *26*, 1343–1345.
53. Meyerowitz, E. A, Richterman, A, Gandhi, R. T., Sax, P.E, Transmission of SARS-CoV-2: a review of viral, host, and environmental factors, *Annals of internal medicine*, 2020., doi:10.7326/M20-5008
54. Patel, M.; Chaubey, A.K. Charles, U.P., Jr.; Mlsna, T. Mohan, D. Coronavirus (SARS-CoV-2) in the Environment: Occurrence, Persistence, Analysis in Aquatic Systems and Possible Management. *Sci Total Environ.* **2021** *765*, 765142698, .



55. Bivins, A.; Greaves, J.; Fischer, R.; Yinda, K.C.; Ahmed, W.; Kitajima, M.; Vincent, Munster, J.; Bibby, K. Persistence of SARS-CoV-2 in Water and Wastewater. *Environ. Sci. Technol. Lett.*, **2020**, *7*, 937–942.
56. van Doremalen, N.; Bushmaker T.; Morris, D.H.; Holbrook, M.G. Gamble, A. Williamson, B.N. Aerosol and surface stability of SARS-CoV-2 as compared with SARS-CoV-2, *New Engl. J. Med.* **2020**, *382*, 1564–1567.
57. Fears, A.C.; Klimstra, W.B.; Duprex, P.; Hartman, A.; Weaver, S.C.; Plante, K.C.; Mirchandani, D.; Plante, J.A.; Aguilar, P.V.; Fernández, D.; et al. Comparative dynamic aerosol efficiencies of three emergent corona viruses and the unusual persistence of SARS-CoV-2 in aerosol suspensions. *medRxiv* **2020**. <https://doi.org/10.1101/2020.04.13.20063784>.
58. Chin, A.W.H.; Chu, J.T.S.; Perera, M.R.A.; Hui, K.P.Y.; Yen, H.; Chan, M.C.W. Stability of SARSCoV-2 in different environmental conditions. *Lancet Microbe* **2020**, *1*, e10.
59. Kasloff, S.B.; Strong, J.E.; Funk, D.; Cutts, T.A. Stability of SARS-CoV-2 on Critical Personal Protective Equipment. *medRxiv* **2020**, <https://doi.org/10.1038/s41598-020-80098-3>.
60. Riddell, S.; Goldie, S.; Hill, A.; Eagles, D.; Trevor; Drew, W. The effect of temperature on persistence of SARS-CoV-2 on common surfaces. *Virol. J.* **2020**, *17*, 145. <https://doi.org/10.1186/s12985-020-01418-7>.
61. Pottage, T.; Garratt, I.; Onianwa, O.; Spencer, A.; Paton, S.; Verlander, N.Q.; Dunning, J.; Bennett, A. A comparison of persistence of SARS-CoV-2 variants on stainless steel. *J. Hosp. Infect.* **2021**, *114*, 163–166.
62. Morris, D.H.; Yinda, K.C.; Gamble, A.; Rossine, F.W.; Huang, Q.; Bushmaker, T.; Fischer, R.J.; Matson, M.J.; van Doremalen, N.; Vikesland, P.J.; et al. 2020. The effect of temperature and humidity on the stability of SARS-CoV-2 and other enveloped viruses. *bioRxiv*, **2020**. <https://doi.org/10.1101/2020.10.16.341883>.
63. Cozad, A.; Jones, R.D. Disinfection and the prevention of infectious disease. *Am. J. Infect. Control*, **2003**, *31*, 243–254.
64. Humberto, P. Antimicrobial Polymers with Metal Nanoparticles. *Int. J. Mol. Sci.* **2015**, *16*, 2099–2116.
65. Lee, K.; Yoon, H.; Ahn, C.; Park, J.; Jeon, S. Strategies to improve the photocatalytic activity of TiO<sub>2</sub>: 3D nanostructuring and heterostructuring with graphitic carbon nanomaterials. *Nanoscale*, **2019**, *11*, 7025–7040.
66. Kris, O.; Dowd, K.; Nair, M.; Parnia, F.; Snehamol, M.; Grant, J.; Moran, R.; Bartlett, J.; Bird, J.; Pillai, S.C. Face Masks and Respirators in the Fight Against the COVID-19 Pandemic: A Review of Current Materials, Advances and Future Perspectives. *Materials*, **2020**, *13*, 3363.
67. Pemmda, R.; Zhu, X.; Dash, M.; Zhou, Y.; Ramakrishna, S.; Peng, X.; Thomas, V.; Jain, S.; Nanda, H.S. Science-Based Strategies of Antiviral Coatings with Viricidal Properties for the COVID-19 Like Pandemics. *Materials*, **2020**, *13*, 4041.
68. Meguid, S.A.; Elzaabalawy, A. Potential of combating transmission of COVID-19 using novel self-cleaning superhydrophobic surfaces: Part I—Protection strategies against fomites. *Int. J. Mech. Mater. Des.* **2020**, *16*, 423–431.
69. Mallakpour, S.; Azadi, E.; Hussain, C.M. Recent breakthroughs of antibacterial and antiviral protective polymeric materials during COVID-19 pandemic and after pandemic: Coating, packaging and textile applications. *Curr. Opin. Colloid Interface Sci.* **2021**, *55*, 101480.
70. Zhou, J.; Hu, Z.; Zabihi, F.; Chen, Z.; Zhu, M. Progress and Perspective of Antiviral Protective Material, Advanced Fiber. *Materials* **2020**, *2*, 123–139.
71. Salam, A.; Hassan, T.; Jabri, T.; Riaz, S.; Khan, A.; Iqbal, K.M.; Khan, S.; Wasim, M.; Shah, M.R.; Khan, M.Q.; et al. Electrospun Nanofiber-Based Viroblock/ZnO/PAN Hybrid Antiviral Nanocomposite for Personal Protective Applications. *Nanomaterials*, **2021**, *11*, 2208.
72. Balasubramaniam, B.; Prateek; Ranjan, S.; Saraf, M.; Kar, P.; Singh, S.P.; Thakur, V.K.; Singh, A.; Gupta, R.K. Antibacterial and Antiviral Functional Materials: Chemistry and Biological Activity toward Tackling COVID-19-like Pandemics. *ACS Pharmacol. Transl. Sci.* **2021**, *4*, 8–54.
73. Erkoc, P.; Ulucan-Karnak, F. Nanotechnology-Based Antimicrobial and Antiviral Surface Coating Strategies. *Prosthesis*, **2021**, *3*, 25–52.
74. Raza, Z.A.; Taqi, M.; Tariq, M.R. Antibacterial agents applied as antivirals in textilebased PPE: A narrative review. *J. Text. Institute*. <https://doi.org/10.1080/00405000.2021.1889166>.
75. Karim, N.; Afroj, S.; Lloyd, K.; Oaten, L.C.; Andreeva, D.V.; Carr, C.; Farmery, A.D.; Kim, Il.; Kostya, N.S.; Sustainable Personal Protective Clothing for Healthcare Applications: A Review. *ACS Nano*. <https://doi.org/10.1021/acsnano.0c05537>.
76. Mallakpour, S.; Azadi, E.; Hussain, C.M. The latest strategies in the fight against the COVID-19 pandemic: The role of metal and metal oxide nanoparticles, *New, J. Chem.* **2021**, *45*, 6167.
77. Govind, V.; Bharadwaj, S.; Sai Ganesh, M.R.; Vishnu, J.; Karthik, V.S.; Shankar, B.; Rajesh, R. Antiviral properties of copper and its alloys to inactivate COVID-19 virus: A review. *Biomaterials*, **2021**, *34*, 1217–1235. <https://doi.org/10.1007/s10534-021-00339-4>.
78. Chiome, T.J.; Srinivasan, A. Use of antiviral nanocoating in personal protective wear, *Int. J. Health Allied Sci.* **2020**, *9*, S62–S67.
79. Borkow, G.; Zhou, S.S.; Page, T.; Gabbay, J. A Novel Anti-Influenza Copper Oxide Containing Respiratory Face Mask. *PLoS ONE* **2010**, *5*, e11295.
80. Zhong, H.; Zhu, Z.; Lin, J.; Cheung, C.F.; Vivien; Lu, L.; Yan, F.; Chan, Ch.; Li, G. Reusable and Recyclable Graphene Masks with Outstanding Superhydrophobic and Photothermal Performances, *ACS Nano*, **2020**, *14*, 6213–6221 <https://doi.org/10.1021/acsnano.0c02250>.
81. Nakamura, S.; Sato, M.; Sato, Y.; Ando, N.; Takayama, T.; Fujita, M.; Ishihara, M. Synthesis and Application of Silver Nanoparticles (Ag NPs) for the Prevention of Infection in Healthcare Workers. *Int. J. Mol. Sci.* **2019**, *20*, 3620. <https://doi.org/10.3390/ijms20153620>.

82. Pollini, M.; Paladini, F.; Licciulli, A.; Maffezzoli, A.; Sannino, A.; Nicolais, L. Antibacterial natural leather for application in the public transport system. *J. Coat. Technol. Res.* **2013**, *10*, 239–245.
83. Hasan, J.; Xu, Y.; Yarlagadda, T.; Schuetz, M.; Spann, K.; Yarlagadda, P.K.D.V. Antiviral and Antibacterial Nanostructured Surfaces with Excellent Mechanical Properties for Hospital Applications. *ACS Biomater. Sci. Eng.* **2020**, *6*, 3608–3618.
84. Murugesan, P.; Moses, J.A.; Anandharamakrishnan, C. Photocatalytic disinfection efficiency of 2D structure graphitic carbon nitride-based nanocomposites: A review. *J. Mater. Sci.* **2019**, *54*, 12206–12235.
85. Rtimi, S.; Sanjines, R.; Andrzejczuk, M.; Pulgarin, C.; Kulik, A.; Kiwi J., Innovative transparent non-scattering TiO<sub>2</sub> bactericide thin films inducing increased E. coli cell wall fluidity. *Surf. Coat. Technol.* **2014**, *254*, 333–343.
86. Djurišić, A.B.; Leung, Y.H.; Ng, A.M.C.; Xu, X.Y.; Lee, P.K.H.; Degger, N.; Wu, R.S.S. Toxicity of metal oxide nanoparticles: Mechanisms, characterization, and avoiding experimental artefacts. *Small.* **2015**, *11*, 26–44.
87. Kim, J.Y.; Lee, C.; Cho, M.; Yoon, J. Enhanced inactivation of E. coli and MS-2 phage by silver ions combined with UV-A and visible light irradiation. *Water Res.* **2008**, *42*, 356–362.
88. Xia, D.H.; Hu, L.L.; Wang, Y.C. Immobilization of facet-engineered Ag<sub>3</sub>PO<sub>4</sub> on mesoporous Al<sub>2</sub>O<sub>3</sub> for efficient industrial waste gas purification with indoor LED illumination. *Appl. Catal. B Environ.* **2019**, *256*, 117811.
89. Zhao, H.N.; Guan, X.Y.; Zhang, F. Rational design of a bismuth oxyiodide (Bi/BiOI- xI) catalyst for synergistic photothermal and photocatalytic inactivation of pathogenic bacteria in water. *J. Mater. Sci.* **2021**, *100*, 110–119.
90. Raut, A.; Yadav, H.; Gnanamani, A.; Pushpavanam, S.; Pawar, S. Synthesis and characterization of chitosan-TiO<sub>2</sub>: Cu nanocomposite and their enhanced antimicrobial activity with visible light. *Colloids Surf. B: Biointerfaces*, **2016**, *148*, 566–575.
91. Hosseini-Sarvari, M.; Jafari, F.; Mohajeri, A.; Hassani, N. Cu<sub>2</sub>O/TiO<sub>2</sub> nanoparticles as visible light photocatalyst concerning C(sp<sup>2</sup>)-P bond formation. *Catal. Sci. Technol.* **2013**, *8*, 1–3, doi:10.1039/c8cy00822a
92. Cao, Y.; Zi, T.; Zhao, X.; Ren, Q.; Fang, J.; Li, W.; Ai-Dong, Enhanced visible light photocatalytic activity of Fe<sub>2</sub>O<sub>3</sub> modified TiO<sub>2</sub> prepared by atomic layer deposition. *Sci. Rep.* **2020**, *10*, 13437, .
93. Patil, S.; Shivaraj, B.; Patil, B.; Ganganagappa, N.; Reddy, K.R.; Anjanapura, Raghu, V.; Reddy, C.V. Recent progress in metal-doped TiO<sub>2</sub>, non-metal doped/codoped TiO<sub>2</sub> and TiO<sub>2</sub> nanostructured hybrids for enhanced photocatalysis. *Int. J. Hydrog.* **2020**, *45*, 7764–7778.
94. Zhou, J.; Tian, G.; Chen, Y.; Wang, J.; Cao, X.; Shi, Y.; Pan, K.; Fu, H. Synthesis of hierarchical TiO<sub>2</sub> nanoflower with anatase rutile heterojunction as Ag support for efficient visible-light photocatalytic activity. *Dalton Trans.* **2013**, *42*, 11242e51.
95. Coto, M.; Divitini, G.; Dey, A.; Krishnamurthy, S.; Ullah, N.; Ducati, C.; Kumar, R.V. Tuning the properties of a black TiO<sub>2</sub>-Ag visible light photocatalyst produced by a rapid one-pot chemical reduction. *Mater. Today Chem.* **2017**, *4*, 142e9.
96. Park, By.; Lee, Ch.; Chung, Ky. Visible Light Photocatalytic Activity of Thin Film Coated on Polycarbonate Surface with N- and Ni-Co doped TiO<sub>2</sub> Photocatalyst. *Catalysts* **2020**, *10*, 1237.
97. Etacheria, V.; di Valentin, C.; Schneider, J.; Bahnemann, D.; Suresh; Pillai, C. Visible-light activation of TiO<sub>2</sub> photocatalysts: Advances in theory and experiments. *J. Photochem. Photobiol. C: Photochem. Rev.* **2015**, *25*, 1–29.
98. Chuaicham, C.; Xiong, Y.; Sekar, K.; Chen, W.; Zhang, L.; Ohtani, B.; Dabo, I.; Sasaki, K. A promising Zn-Ti layered double hydroxide/Fe-bearing montmorillonite composite as an efficient photocatalyst for Cr (VI) reduction: Insight into the role of Fe impurity in montmorillonite. *Appl. Surf. Sci.* **2021**, *546*, 148835, 2021.
99. Chuaicham, C.; Sekar, K.; Xiong, Y.; Balakumar, V.; Mittraphab, Y.; Shimizu, K.; Ohtani, B.; Dabo, I.; Sasaki, K. Single-step synthesis of oxygen-doped hollow porous graphitic carbon nitride for photocatalytic ciprofloxacin decomposition. *Chem. Eng. J.* **2021**, *425*, 130502.
100. Hu, C.; Guo, J.; Qu, J.; Hu, X.; Photocatalytic Degradation of Pathogenic Bacteria with AgI/TiO<sub>2</sub> under Visible Light Irradiation, *Langmuir*. **2007**, *23*, 4982–4987.
101. Guiying, L.; Nie, X.; Chen, J.; Jiang, Q.; An, P.T.; Wong, P.K.; Zhang, H.; Zhao, H.; Yamashita, H. Enhanced visible-light-driven photocatalytic inactivation of E. coli using g-C<sub>3</sub>N<sub>4</sub>/TiO<sub>2</sub> hybrid photocatalyst synthesized using a hydrothermal-calcination approach. *Water Res.* **2015**, *86*, 17–24.
102. Ghodsi, S.; Esrafl, A.; Sobhi, H.R.; Kalantary, R.R.; Gholami, M.; Maleki, R. Synthesis and application of g-C<sub>3</sub>N<sub>4</sub>/ Fe<sub>3</sub>O<sub>4</sub>/Ag nanocomposite for the efficient photocatalytic inactivation of Escherichia coli and Bacillus subtilis bacteria in aqueous solutions. *AMB Express*, **2021**, *11*, 161.
103. Saravanan, A.; Kumar, P.S.; Jeevanantham, S.; Karishma, S.; Kiruthika, A.R. Photocatalytic disinfection of micro-organisms: Mechanisms and applications. *Environ. Technol. Innov.* **2021**, *24*, 101909.
104. Wang, W.; Huang, G.; Jimmy, Yu, C.; Wong, P.K. Advances in photocatalytic disinfection of bacteria: Development of photocatalysts and mechanisms. *J. Environ. Sci.* **2015**, *34*, 232–247.
105. An; T.; Zhao, H.; Wong; P.K. *Advances in Photocatalytic Disinfection*; Springer: Berlin, Germany, 2017; ISBN 978–3–662–53494–6.
106. Irshad, M.A.; Nawaz, R.; Rehman, M.Z.u.; Adrees, M.; Rizwan, M.; Ali, S.; Ahmad, S.; Tasleem, S. Synthesis characterization and advanced sustainable applications of titanium dioxide nanoparticles: A review, *Ecotoxicol. Environ. Saf.* **2021**, *212*, 111978.
107. Solano, R.; Patino-Ruiz, D.; Herrera, A. Preparation of modified paints with nano-structured additives and its potential applications. *Nanomater. Nanotechnol.* **2020**, *10*, 1–17.
108. Roopan, S.M.; Bharathi, A.; Prabhakarn, A.; Rahuman, A.A.; Velayutham, K.; Rajakumar, G.; Padmaja, R.D.; Lekshmi, M.; Madhumitha, G.; Efficient phyto-synthesis and structural characterization of rutile TiO<sub>2</sub> nanoparticles using Annona squamosa peel extract. *Spectrochim. Acta A Mol. Biomol. Spectrosc.* **2012**, *98*, 86–90.

109. Vembu, S.; Vijayakumar, S.; Nilavukkarasi, M.; Vidhya, E.; Punitha, V.N. Phytosynthesis of TiO<sub>2</sub> nanoparticles in diverse applications: What is the exact mechanism of action? *Sensors* **2022**, *3*, 100161, 2022.
110. Rajeshkumar, S.; Santhoshkumar, J.; Jule, L.T.; Ramaswamy, K. Phytosynthesis of Titanium Dioxide Nanoparticles Using King of Bitter *Andrographis paniculata* and Its Embryonic Toxicology Evaluation and Biomedical Potential. *Bioinorg. Chem. Appl.* **2021**. <https://doi.org/10.1155/2021/6267634>.
111. Thakur, B.K.; Kumar, A.; Kumar, D. Green synthesis of titanium dioxide nanoparticles using *Azadirachta indica* leaf extract and evaluation of their antibacterial activity. *South Afr. J. Bot.* **2019**, *124*, 223–227.
112. Cheng, X.; Yu, X.; Xing, Z.; Yang, L. Synthesis and characterization of N-doped TiO<sub>2</sub> and its enhanced visible-light photocatalytic activity. *Arabian J. Chem.* **2016**, *2*, S1706–S1711.
113. Than, L.D.; Luong, N.S.; Ngo, V.D.; Tien, N.M.; Dung, T.N.; Nghia, N.M.; Loc, N.T.; Thu, V.T.; Lam, T.D. Highly Visible Light Activity of Nitrogen Doped TiO<sub>2</sub> Prepared by Sol–Gel Approach. *J. Electron. Mater.* **2017**, *46*, 1.
114. Reda, S.M.; Khairy, M.; Mousa, M.A.; Photocatalytic Activity of Nitrogen and Copper Doped TiO<sub>2</sub> Nanoparticles Prepared by Microwave-Assisted Sol-Gel Process. *Arabian J. Chem.* **2020**, *13*, 86–95.
115. Nassoko, D.; Li, Ya.; Wang, H.; Li, Ji.; Li, Yu.; Yu, Y. Nitrogen-doped TiO<sub>2</sub> nanoparticles by using EDTA as nitrogen source and soft template: Simple preparation, mesoporous structure, and photocatalytic activity under visible light. *J. Alloys Compd.* **2012**, *540*, 228–235.
116. Mehdizadeh, P.; Tavangar, Z.; Shabani, N.; Hamadian, M. Visible Light Activity of Nitrogen-Doped TiO<sub>2</sub> by Sol-Gel Method Using Various Nitrogen Sources. *J. Nanostruct. Spring.* **2020**, *10*, 307–316.
117. Akhavan, O.; Azimirad, R.; Safa, S.; Larijani, M.M. Visible light photo-induced antibacterial activity of CNT-doped TiO<sub>2</sub> thin films with various CNT contents. *J. Mater. Chem. J. Mater. Chem.* **2010**, *20*, 7386–7392.
118. Shafei, A.; S. Sheibani, Visible light photocatalytic activity of Cu doped TiO<sub>2</sub>-CNT nanocomposite powder prepared by sol-gel method. *Mater. Res. Bulletin* **2019**, *110*, 198–206.
119. Mohammad, R.M.; Ahmed, D.S.; Mohammed, M.K.A. Synthesis of Ag-doped TiO<sub>2</sub> nanoparticles coated with carbon nanotubes by the sol–gel method and their antibacterial activities. *J. Sol-Gel Sci. Technol.* **2019**, *90*, 498–509.
120. Conga, Y.; Li, X.; Qin, Y.; Dong, Z.; Yuan, G.; Cui, Z.; Lai, X. Carbon-doped TiO<sub>2</sub> coating on multiwalled carbon nanotubes with higher visible light photocatalytic activity. *Appl. Catal. B* **2011**, *107*, 128–134.
121. Markowska-Szczupak, A.; Ulfig, K.; Grzmil, B.; Antoni, Morawski, W.; A preliminary study on antifungal effect of TiO<sub>2</sub>-based paints in natural indoor light. *Pol. J. Chem. Technol.* **2010**, *12*, 53–57.
122. de Amorim, S.M.; Sapatieri, J.C.; Moritza, D.E.; di Domenico, M.; Laqua, L.A.d.; Moura-Nickel, C.D.; Falcão Aragão, G.M.; Moreira, R.d.P.M. Antifungal and Photocatalytic Activity of Smart Paint Containing Porous Microspheres of TiO<sub>2</sub>. *Mater. Res.* **2019**, *22*, 6.
123. Kumaravel, V.; Keerthi; Nair, M.; Mathew, S.; Bartlett, J.; James; Kennedy, E.; Hugh; Manning, G.; Barry; Whelan, J.; Nigel; Leyland, S.; Suresh; Pillai, C.; Antimicrobial TiO<sub>2</sub> nanocomposite coatings for surfaces, dental and orthopaedic implants. *Chem. Eng.* **2021**, *416*, 129071.
124. Jašková, V.; Hochmannová, L.; Jarmila VytLasová, TiO<sub>2</sub> and ZnO Nanoparticles in Photocatalytic and Hygienic Coatings. *Int. J. Photoenergy*. 2013. <https://doi.org/10.1155/2013/795060>.
125. Vera; Sousa, M.; Célia; Manaia, M.; Mendes, A.; Olga; Nunes, C. Photoinactivation of various antibiotic resistant strains of *Escherichia coli* using a paint coat. *J. Photochem. Photobiol.* **2013**, *251*, 148–153.
126. Zacarias, S.M.; Marchetti, S.; Alfano, O.M.; de los Milagros Ballari, M. Photocatalytic paint for fungi growth control under different environmental conditions and irradiation sources. *J. Photochem. Photobiol. A Chem.* **2018**, *364*, 76–87.
127. Cheng, Ch.; Sun, De.; Chu, We.; Tseng, Ya.; Ho, Ha.; Wang, Ji.; Chung, Pe.; Chen, Ji.; Tsai, P.; Lin, Ni.; Yu, Me.; et al. The effects of the bacterial interaction with visible-light responsive titania photocatalyst on the bactericidal performance. *J. Biomed. Sci.* **2009**, *16*, 7.
128. Reddy, P.V.L.; Kavitha, B.; Reddy, P.A.K.; Kim, Ki. TiO<sub>2</sub>-based photocatalytic disinfection of microbes in aqueous media: A review. *Environ. Res.* **2017**, *154*, 296–303.
129. Markowska-Szczupak, A.; Ulfig, K.; Morawski, A.W. The application of titanium dioxide for deactivation of bioparticulates: An overview. *Catalyst* **2011**, *169*, 249–257.
130. Tornero, ACF; Blasco, MG; Azqueta, MC, Antimicrobial ecological waterborne paint based on novel hybrid nanoparticles of zinc oxide partially coated with silver. *Prog Org Coatings*, **2008**, *121*, 130–141
131. Bonnefond, A.; González, E.; Asua, J.M.; Leiza, J.R.; Ieva, E.; Brinati, G.; Carella, S.; Marrani, A.; Veneroni, A.; Kiwi, J.; et al. Stable Photocatalytic Paints Prepared from Hybrid Core-Shell Fluorinated/Acrylic/TiO<sub>2</sub> Waterborne Dispersions. *Crystals*, **2016**, *6*, 136.
132. Vignesh Kumaravel , Keerthi M. Nair, Snehamol Mathew , John Bartlett, James E. Kennedy, Hugh G. Manning , Barry J. Whelan , Nigel S. Leyland , Suresh C. Pillai, Antimicrobial TiO<sub>2</sub> nanocomposite coatings for surfaces, dental and orthopaedic implants, *Chemical Engineering Journal*, **2021**, *416*, 129071
133. Koli, V.B.; Dhodamani, A.G.; Delekar, S.G.; Pawar, S.H. In situ sol-gel synthesis of anatase TiO<sub>2</sub>-MWCNTs nanocomposites and their photocatalytic applications. *J. Photochem. Photobiol.* **2017**, *333*, 40–48.

134. Yadav, H.M.; Otari, S.V.; Koli, V.B.; Mali, S.S.; Hong, C.K.; Pawar, S.H.; Delekar, S.D. Preparation and characterization of copper-doped anatase TiO<sub>2</sub> nanoparticles with visible light photocatalytic antibacterial activity. *J. Photochem. Photobiol.* **2014**, *280*, 32–38.
135. Zuccheri, T.; Colonna, M.; Stefanini, I.; Santini, C.; di Gioia, D. Bactericidal Activity of Aqueous Acrylic Paint Dispersion for Wooden Substrates Based on TiO<sub>2</sub> Nanoparticles Activated by Fluorescent Light. *Materials*. **2013**, *6*, 3270–3283.
136. Darade, M.M.; Pawar, S.H.; Pawaskar, S.R. Antifungal activities and photo disinfection of TiO<sub>2</sub> nano composite paints for health care in building. *Int. J. Sci. Eng. Res.* **2021**, *12*, 10–15.
137. Silvia Bonetta, Sara Bonetta, Francesca Motta, Alberto Strini, Elisabetta Carraro, Photocatalytic bacterial inactivation by TiO<sub>2</sub>-coated surfaces, *AMB Express*, **2013**, *3*, 59.
138. Salvadores, F.; Reli, M.; Alfano, O.M.; Koci, K.; de los Milagros Ballari, M. Efficiencies Evaluation of Photocatalytic Paints Under Indoor and Outdoor Air Conditions. *Front. Chem.* **2020**, *8*, 551710. <https://doi.org/10.3389/fchem.2020.551710>.
139. Seven, O. Solar photocatalytic disinfection of a group of bacteria and fungi aqueous suspensions with TiO<sub>2</sub>, ZnO and Sahara Desert dust. *J. Photochem. Photobiol.* **2004**, *165*, 103–107.
140. Darade, M. Antimicrobial Activities of TiO<sub>2</sub> Nano-Powder Based Surface Coatings for Health Care Applications. *Jetir*. **2019**, *6*, 1006–1013.
141. Van Driel, B.A.; van den Berg, K.J.; Smout, M.; Dekker, N.; Kooyman, P.J.; Dik, J. Investigating the effect of artists' paint formulation on degradation rates of TiO<sub>2</sub>-based oil paints. *Herit Sci.* **2018**, *6*, 21.
142. Morsch, S.; Birgit; van Driel, A.; Jan van den Berg, K.; Dik, J. Investigating the Photocatalytic Degradation of Oil Paint using ATR-IR and AFM-IR. *Appl. Mater. Interfaces*. **2017**, *9*, 10169–10179.
143. van Driel, B.A.; Wezendonk, T.A.; van den Berg, K.J.; Kooyman, P.J.; Gascon, J.; Dik, J. Determination of early warning signs for photocatalytic degradation of titanium white oil paints by means of surface analysis. *Spectrochim. Acta A Mol. Biomol. Spectrosc.* **2017**, *172*, 100–108.
144. Basso, A.; Battisti, A.P.; Moreira, R.d.P.M.; Jose, H.J. Photocatalytic effect of addition of TiO<sub>2</sub> to acrylic-based paint for passive toluene degradation. *Environ. Technol.* **2020**, *41*, <https://doi.org/10.1080/09593330.2018.1542034>.
145. Ren, Y.; Cai, J.; Cheung, H.; Shao, H.; Au, K.; Chow, T.; Wen, W.; Ling, L.; Chen, S. Controlling microbial activity on walls by a photocatalytic nanocomposite paint: A field study. *Am. J. Infect. Control*. **2021**, *00*, 1–8.
146. Lindblad, M.; Tano, E.; Lindahl, C.; Huss, F.; Ultraviolet, C. Decontamination of a hospital room: Amount of UV light needed. *Burns*. **2020**, *46*, 842–849.
147. Jelden, K.C.; Gibbs, S.G.; Smith, P.W. Comparison of hospital room surface disinfection using a novel ultraviolet germicidal irradiation (UVGI) generator. *J. Occup. Environ. Hyg.* **2016**, *13*, 690–698.